

Sudan University of Science and Technology

College of Graduate studies

Synthesis and Characterization of Zinc Oxide

Nanostructure at Low Temperature

تخليق وتشخيص اوكسيدالزنك النانوي في درجة حرارة منخفضة

A Thesis Submitted in Partial Fulfillment for the Requirements of the Degree of
Master of Science in Chemistry

By

Fatin Ali Alawad Mohammed Ali

(B.Sc. Honours in Scientific laboratories)

Supervisor: Dr. Elfatih Ahmed Hassan

June. 2016

استفتاح

بِسْمِ اللّٰهِ الرَّحْمٰنِ الرَّحِیْمِ

(قل لو كان البحر مدادا لكلمات ربي لنفد البحر قبل ان تنفد

كلمات ربي ولو جئنا بمثله مددا)

(الكهف 109)

صدق الله العظيم

Dedication

This thesis is dedicate to:

My parents

My brother

Acknowledgement

All praise is due to Allah the most Gracious the most Merciful for giving me health and patience to accomplish this work.

I would like to express my deep thanks to my supervisor **Dr. Elfatih Ahmed Hassan** for his continuous encouragement and support

Also I would like to thank **Mr.Abu Aleze Khalid Modawey** Who provided assistance with some parts of characterization exiperminte

I would like to thank **prof.Omer Salih Mohamed Nour** who give me some knowledge about the article of the research

Abstract

On this study Zinc oxide nanoparticles were prepared by hydrothermal method at low temperature (60°C), also ZnO nanoparticles were grown as a thin film on glass substrate. In addition, a zinc oxide nanoparticles grown as a thin film on glass substrate was coated with another layer of CuO nanoparticles. The Shape and size of these grown nanostructures were then characterized by UV absorption, SEM, and EDX technique. Band gap of ZnO was calculated from UV absorption measurement and it was found to be 3.66eV, a value that exceeds, the reported value of ZnO band gap namely 3.37eV. The increase of band gap of the prepared ZnO was attributed to presence of Si, Mg, Ca, Al impurities which were evidence from EDX analysis. Particle size of ZnO on two dimensions (x, y) and the distance between crystals was estimated from SEM analysis

مستخلص البحث

في هذه الدراسة تم تحضير اوكسيد الزنك النانوي بالطريقة الهيدروثيرمية في درجة حرارة منخفضة (60 درجة مئوية)، ايضا تمتنعمة اوكسيد الزنك النانوي في شكل طبقة رقيقة علي الزجاج .بالاضافة الي انه تم تغطية طبقة اوكسيد الزنك النانوي النامية علي شريحة الزجاج بواسطة طبقة اخري من اوكسيد النحاس النانوي .تم تشخيص حجم وشكل هذه الجزيئات النانوية بواسطة تقنية مطيافية امتصاص الاشعة فوق البنفسجية ،مجهرالمسح الالكتروني ومطيافية تشتت الاشعة السينية .تم استخدام تقنية امتصاصية الاشعة فوق البنفسجية لحساب قيمة فجوة الطاقة لاوكسيد الزنك ووجد انها تساوي 3.66الكترن .فولت والتي تتجاوزالقيمة المحددة لفجوة الطاقة والتي تبلغ 3.37 الكترن فولت . هذا التغير في فجوة الطاقة لاوكسيد الزنك النانوي المحضريعزي لوجودشوائب من السليكون،الماغنيسيوم ،الكالسيوم ،الالمونيم التي ظهرت في تحليل مطيافية تشتت الاشعة السينية . حجم جزيئات اوكسيد الزنك النانوي في بعدين (x,y) والمسافة بين الجزيئات تم تقديرها بواسطة مجهر المسح الالكتروني

Table of contents

Contents	Pages
Holy Quran verse	I
Dedication	II
Acknowledgement	III
Abstract	IV
مستخلص البحث	V
Table of contents	VI- VIII
List of tables	IX
List of figures	X
Chapter One-Introduction	
1.1 What is nanotechnology?	1
1.2 Classification of nanoparticle	2
1.2.1 One dimension nanoparticle	2
1.2.2 Two dimension nanoparticle	2
1.2.3 Three dimension nanoparticles	3
1.3 Conditions of preparation nanostructure	4
1.4 Why is metal oxides	4
1.5 Techniques of synthesis of nanoparticles (top-down and bottom up)	5
1.6 Zinc oxide nanostructures—synthesis methods	6
1.7 Some approaches of preparation of nanoparticle	7
1.7.1 ZnO nanostructures through	7
1.7.2 Milling Process	8
1.7.3 Chemical bath deposition	10
1.8 Crystal structure of ZnO	10
1.9 Nanoparticle of ZnO	11

1.10 Some factors affect on the morphology of ZnO nanoparticle	12
1.11 Characteraization of zinc oxide nanoparticle	16
1.11.1 X-ray diffraction analysis	16S
1.11.2 Transmission Electron Microscopy	17
1.11.3 FTIR spectroscopy	18
1.11.4 UV-Visible spectroscopy	19
1.11.5 DSC analysis	22
1.12 Some applications of ZnO nanostructure	23
1.13 literature review	24
1.14 Objectives of study	29
Chapter Two– Experimental	
2.1 Chemicals	30
2.2 Instrumentations and equipments	30
2.2.1 Instrumentations	30
2.2.2 Equipments	30
2.3 Preparation procedure	31
2.3.1 Seed solution for ZnO nanostructure growth	31
2.3.2 The aqueous chemical growth solution for the ZnO	31
2.3.3 Standard cleaning procedure	31
2.3.4 Coating ZnO with CuO	32
2.4 Characteraization method	32
2.4.1 Uv-vis absorption spectrophotometer test	32
Chapter Three-Results and Discussion	
3.1 UV –VIS absorption technique	33
3.1.1 The optical characterization of powder sample of ZnO recorded on Uv- Vis absorption spectrophotometer	33
3.2 SEM technique	35

3.3 EDX technique	36
3.3.1 SEM plus EDX for ZnO on glass	36
3.3.2 SEM plus EDX result for ZnO coating by CuO	37
3.5 Effect of temperature on shape and size of ZnO nanoparticle	38
3.6 Conclusion	39
References	40

List of table

Contents	Pages
Tables	
Table 1. Morphologies obtained using different templates	7

List of figures

Contents	Pages
Figures	
Figure 1. 1. The hexagonal wurtzite structure model of ZnO.	11
Figure 1.2. TEM micrographs of ZnO nanoparticles	13
Figure 1.3. shows XRD diffraction pattern of ZnO nanoparticles	17
Figure 1.4. TEM images of ZnO nanoparticles (a, b) and its selected area electron diffraction image (c).	18
Figure 1.5. FTIR spectra of ZnO nanoparticles	19
Figure 1. 6(a). Absorption of ZnO nanoparticles as a function of wavelength	20
Figure 1. 6(b). Variation of $(ahv)^2$ with hv for ZnO nanoparticles as a function of wavelength at $n=1/2$	21
Figure 1. 7 DSC curve of ZnO nanoparticles	22
Figure 1.8. Worldwide consumption of zinc oxide.	23
Figure 1.9 Schematic representation of application of ZnO	24
Figure 3.1. Absorption of ZnO nanoparticles as a function of wavelength	33
Figure 3.2 Variation of $(ahv)^2$ with hv for ZnO nanoparticles as a function of wavelength at $n = 1/2$	34
Figure 3.3. SEM image of ZnO on normal glass	35
Figure 3.4 SEM and EDX of ZnO on glass	36
Figure 3.5 SEM plus EDX of ZnO coating by CuO	37
Figure 3.6 SEM image for ZnO Coating by CuO on normal glass	38

Chapter one

Introduction

Chapter one

1. Introduction

1.1 What is nanotechnology?

The prefix “Nano” has found in last decade an ever-increasing application to different fields of the knowledge. Nanoscience, nanotechnology, nanomaterials are only a few of the new nano-containing terms in scientific reports, in popular books as well as in newspapers and that have become familiar to a wide public, even of non-experts. The prefix comes from the ancient Greek *νάνος* through the Latin *nanus* meaning literally dwarf and, by extension, very small. Within the convention of International System of Units (SI) it is used to indicate a reduction factor of 10^9 times. So, the nanosized world is typically measured in nanometers (1 nm corresponding to 10^{-9} m) and it encompasses systems whose size is above molecular dimensions and below macroscopic ones (generally larger than 1 nm and below 100 nm)

Nanotechnology is the science of the small; the very small. It is the use and manipulation of matter at a tiny scale. At this size, atoms and molecules work differently, and provide a variety of surprising and interesting uses. Nanotechnology and Nanoscience studies have emerged rapidly during the past years in a broad range of product domains. It provides opportunities for the development of materials, including those for medical applications, where conventional techniques may reach their limits. Nanotechnology should not be viewed as a single technique that only affects specific areas. Although often referred to as the ‘tiny science’, nanotechnology does not simply mean very small structures and products. Nanoscale features are repeatedly incorporated into bulk materials and large surfaces. Nanotechnology represents the design, production and application of materials at atomic, molecular and macromolecular scales, in order to produce new nanosized materials. Pharmaceutical nanoparticles are defined as solid, submicron-sized (less than 100 nm in diameter) drug carrier that may or may not be biodegradable. The term nanoparticle is a combined name for both nanospheres and nanocapsules. Nanospheres are matrix system in which drug is uniformly dispersed, while nanocapsules are the system in which the drug is surrounded by a unique polymeric membrane. This systemic review focuses on Classification, method of preparation, Characterization, application, health prospective and Pharmacological aspects of nanoparticles ^[1]

In recent years the research on nanostructures of different materials and their use for devices and systems have been increasing. The reason for this is the unique properties of nanostructures that are advantageous over bulk materials. An example of this is the dependence of the chemical and physical properties of nanostructures on size. For example the relatively large surface area to volume ratio renders surface effects and forces to dominate over other forces. Such property would lead to potential use of some nanomaterials for many applications, like e.g. for sensors. Adding to this the order of size of nanostructures which is similar to many biological analytes and chemical species would render their sensitivity to be quite high even in small volumes. The intensified research on growth and prototype devices based on nanostructures has reached a stage where reproducibility and control of the nanostructures is acceptable for many materials. Many materials are under focus with the potential of developing nano -systems. The optimization of the performance is the main challenge at the moment. [2]

1.2 Classification of nanoparticles

There are various approaches for classification of nanomaterials. Nanoparticles are classified based on one, two and three dimension

1.2.1 One dimension nanoparticles

One dimensional system, such as thin film or manufactured surfaces, has been used for decades in electronics chemistry and engineering. Production of thin films (sizes 1-100nm) or monolayer is now common place in the field of solar cells or catalysis. This thin films are used in different technological applications, including information storage systems, chemical and biological sensors, fibre-optic systems, magneto-optic and optical device.

1.2.2 Two dimension nanoparticles

Carbon nanotubes (CNTs)

Carbon nanotubes are hexagonal network of carbon atoms, 1 nm in diameter and 100 nm in length, as a layer of graphite rolled up into cylinder. CNTs are of two types, single walled carbon nanotubes (SWCNTs) and multi-walled carbon nanotubes (MWCNTs). The small dimensions of carbon nanotubes combined with their remarkable physical, mechanical and electrical properties, make them unique materials. They display metallic or semi conductive properties, depending on the carbon leaf is wound on itself. The current density that nanotubes can carry is extremely high

and can reach one billion amperes per square meter making it a superconductor. The mechanical strength of carbon nanotubes is sixty times greater than best steels. Carbon nanotubes have a great capacity for molecular absorption and offering a three dimensional configuration. Moreover they are chemically and chemically very stable.

1.2.3 Three dimension nanoparticles

Fullerenes (Carbon 60)

Fullerenes are spherical cages containing from 28 to more than 100 carbon atoms, contain C_{60} . This is a hollow ball composed of interconnected carbon pentagons and hexagons, resembling a soccer ball. Fullerenes are class of materials displaying unique physical properties. They can be subjected to extreme pressure and regain their original shape when the pressure is released. These molecules do not combine with each other, thus giving them major potential for application as lubricants. They have interesting electrical properties and it has been suggested to use them in the electronic field, ranging from data storage to production of solar cells. Fullerenes are offering potential application in the rich area of Nano electronics. Since fullerenes are empty structures with dimensions similar to several biological active molecules, they can be filled with different substances and find potential medical application [1]

One-dimensional (1D) semiconductors have attracted enormous attention in recent decades not only for fundamental physical and chemical studies but also for promising applications in various technological areas. Huge scientific efforts have been devoted toward fabricating (1D) nanostructures. Zinc oxide (ZnO) is an II-VI semiconductor material with many interesting properties such as a wide band gap of about 3.37 eV and exciton binding energy of 60 meV both at room temperature. In addition, ZnO provides laser action at room temperature due to electron-hole plasma. This is along with a high piezoelectric tensor owing to the high ionicity nature of the Zn-O bond. Preferentially, ZnO crystallizes in a hexagonal wurtzite crystal structure, space group $P6_3mc$ or C_{6v} . Other crystal structures phases such as rock-salt and zinc-blend are also present metastable crystal forms of ZnO. Among all the attractive properties of ZnO, the excellent optical properties are paving the way for a diversity of optoelectronics applications including white light emitting diodes and field emission devices, despite the fact that a reliable and stable p-type doping essential for p-n junction necessary for electronic and optoelectronic applications is difficult to accomplish.

ZnO nanostructured materials such as nanorods, nanowires, and nanotubes grow mainly along the c-axis of the hexagonal wurtzite crystal structure of ZnO and have recently been reported. On the other hand, nanobelts, nanosprings, and nanohelices have also been demonstrated, and they represent the family of ZnO nanostructures growing along the a-axis.

1.3 Conditions of preparation of nanostructure

The growth of these nanostructures has been performed in two temperature regimes. These are the low temperature wet chemical techniques at temperatures as low as 100 °C and high temperature physical or physio-chemical strategies at temperatures higher than 600°C Both strategies have advantages and disadvantages. For instance, the chemical bath deposition as an example of a wet chemical technique yields a simple two-step growth procedure for well-aligned ZnO nanorods but shows a large presence of defects associated with the photoluminescence of the as-grown samples. A post annealing is essential for obtaining a better near band emission (NBE) for such grown ZnO nanorods arrays (ZNRAs). High temperature growth techniques on the other hand require complex equipment and in many circumstances cannot be utilized for large area deposition. In addition, high temperature techniques cannot be achieved using certain types of substrates, for example, flexible plastic substrates^[3]

1.4 Why is metal oxides?

Among all the functional materials designed at the nanoscale, metal oxides and mixed metal oxides are particularly attractive candidates from a scientific as well as technological point of view. The unique characteristics of metal oxides structured at the nanoscale make them the most diverse class of materials, with properties covering almost all of the aspects of materials science and solid state physics.

Nanoscale metal oxides play an important role in the different fields of nanoscience and nanotechnology, e.g., biology, chemistry, physics, materials science, from electronics to nanomedicine. The preparation of metal oxide nanocrystals can be achieved through many different approaches by either physical or chemical methods. Among them, the surfactant-assisted pathways are the most easily controlled for the size, shape, composition, and phase structure of the resulting nanocrystals. The importance of the surfactant is highlighted by the fact that nanocrystals produced by colloidal routes are generally considered together with the surfactants that coat them. This organic coating allows for additional synthetic flexibility in that

the surfactants can be substituted to different organic molecules with different functional groups or polarity.

Although there have been many new interesting developments in the shape control of metal oxide nanocrystals in the past few years, there is still a great deal of work to be done. Current shape control strategies still rely highly on experimental trial-and-error approaches rather than on rational design of synthetic strategies. The next step should focus on the development of more versatile and reliable but simple synthetic schemes for tailored architecture of nanocrystals with desired components. Concurrently, a better understanding of the guiding principles of crystal growth at the nanoscale level should be pursued. This knowledge will enable further fine tuning of the size, shape, and surfaces, and thus functionalities, of nanocrystals. Additionally, the synthesis of hybrid nanocrystals in which nanocrystals of different shapes and properties are connected together in a single particle is also a fascinating subject. The success in synthesizing such multi-component nanocrystals will open access to a completely novel generation of colloidal structures with prospects of optoelectronic, magnetic, biomedical, photovoltaic, and catalytic applications with high level of performance.

Metal oxide nanocrystals in a variety of shapes such as spheres, cubes, rods, wire, disks, and polypods

1.5 Techniques of synthesis of nanoparticles (top-down and bottom up)

The syntheses of nanoparticles are generally grouped into two broad categories: “bottom up” and “top down”. The process in which materials prepared from atomic precursors assemble to form clusters and subsequently nanoparticles is referred to as “bottom up” approach. Conversely, when the nanoscale is reached by physically disassembling large building blocks, the process is referred to as “top down” approach. The advantage of the physical methods is the possibility to produce a large quantity of nanoparticles, whereas the synthesis of uniform-sized nanoparticles and the control of their size remain very difficult by using the top-down route. The “Bottom up” approach is of primary interest for chemistry and materials science because the fundamental building blocks are atoms; thus colloidal chemical synthetic methods can be utilized to prepare uniform nanocrystals with controlled particle size. In the following, we will concentrate on solution phase synthetic methods that enable a proper shape and size control of metal oxide nanocrystals, methods which include solvothermal/hydrothermal procedures, two-phase routes,

microemulsions, and thermal decomposition. These techniques involve the use of surfactant molecules and, consequently, result in oxide nanocrystals comprising an inorganic core coated with a layer of organic ligand molecules. This organic capping provides electronic and chemical passivation of the surface dangling bonds, prevents uncontrolled growth and agglomeration of the nanoparticles, and permits chemical manipulations of the nanoparticles similarly to large molecules having their solubility and reactivity determined by the nature of the surface ligands [4]

1.6 Zinc oxide nanostructures—synthesis methods

The synthesis methods of different zinc oxide nanostructures can broadly be classified as follows:

a. **Solution phase synthesis:** In the solution phase synthesis, the growth process is carried out in a liquid. Normally aqueous solutions are used and the process is then referred to as hydrothermal growth process. Some of the solution phase synthesis processes are:

1. Zinc Acetate Hydrate (ZAH) derived nano-colloidal sol-gel route
2. ZAH in alcoholic solutions with sodium hydroxide (NaOH) or tetra methyl ammonium hydroxide (TMAH)
3. Template assisted growth
4. Spray pyrolysis for growth of thin films.
5. Electrophoresis

b. **Gas phase synthesis:** Gas phase synthesis uses gaseous environment in closed chambers.

Normally the synthesis is carried out at high temperatures from 500 °C to 1500°C some commonly used gas phase methods are:

1. Vapour phase transport, which includes vapour solid (VS) and vapour liquid solid (VLS) growth
2. Physical vapour deposition
3. Chemical vapour deposition
4. Metal organic chemical vapour deposition (MOCVD).
5. Thermal oxidation of pure Zn and condensation
6. Microwave assisted thermal decomposition

1.7 Some approaches of preparation of nanoparticles

1.7.1 ZnO nanostructures through hydrothermal growth

Nanoparticles. Even though the organometallic synthesis of ZnO nanoparticles in alcoholic medium has received wider acceptance for reasons of faster nucleation and growth as compared to water, still scattered reports of hydrothermal synthesis in aqueous medium are available in synthesized nanoparticles of different morphologies using $ZnCl_2$ and NaOH in a hydrothermal growth process using different organic compounds as template agents. A significant change in the morphology was observed as the synthesis temperature was increased with the particles changing from rod like to polyhedral. It was reported that the morphology also changed with the addition of different organic templates to the reaction mixture when the temperature was maintained at 160 °C. The various morphologies along with the templates used are listed in table1.

Table1.1 Morphologies obtained using different templates.

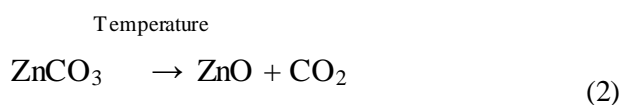
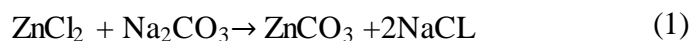
Particle properties

Additives	Morphology	Size (nm)
Tributylamine	Rod-like	200–300
Trimethylamine	Rod-like	100–300
Triethanolamine	Spindle-like	100–300
Diisopropylamine	Rod-like	200–400
Ammonium phosphate	Rod-like	200–500
1, 6-Hexadecanol	Rod-like	300–700
Triethyldiethanol	Rod-like	100–300
Isopropylamine	Rod or sheet-like	
Cyclohexylamine	Sheet-like	300–500
n-Butylamine	Sheet-like	200–400
Ammonium chloride	Sheet	50–200
Hexamethylenetetramine	Snow-flake like	20–50
Ethylene glycol	Ellipse	40–100
Ethanolamine	Polyhedron	50–200

A very simple procedure to prepare ZnO nanoparticles at a very high pH ~14 using tetramethylammonium hydroxide (TMAH) as a precipitating agent was suggested by Musić *al*. Nanoparticles sized from 10 to 20 nm were precipitated at room temperature by adding TMAH to an ethanolic solution of zinc acetate dehydrate. Addition of water to the ethanolic solution prior to adding TMAH yielded ZnO snowflakes. Vishwanathan and Gupta have shown that supercritical water can also be a good reaction medium for the hydrothermal synthesis of ZnO nanoparticles. Spherical ZnO nanoparticles were synthesized by oxidation of zinc acetate in supercritical water in a continuous tubular reactor. Particle size and morphology can be controlled by varying conditions like temperature, pressure or the reaction atmosphere. Nanoparticles with diameters ranging between 39 and 320 nm were synthesized using this method. The synthesis time has been significantly reduced through the use of microwave irradiation and the ZnO nanocrystallites thus formed were observed to be more defective than the ones synthesized over a few hours of hydrolysis. Nanoparticles with inherent defects are capable of exhibiting visible light photocatalysis even without doping with transition metals, which is the normally followed method. [5]

1.7.2 Milling Process

The mechanochemical process is a cheap and simple method of obtaining nanoparticles on a large scale. It involves high-energy dry milling, which initiates a reaction through ball–powder impacts in a ball mill, at low temperature. A “thinner” is added to the system in the form of a solid (usually NaCl), which acts as a reaction medium and separates the nanoparticles being formed. A fundamental difficulty in this method is the uniform grinding of the powder and reduction of grains to the required size, which decreases with increasing time and energy of milling. Unfortunately, a longer milling time leads to a greater quantity of impurities. The advantages of this method are the low production costs, small particle sizes and limited tendency for particles to agglomerate, as well as the high homogeneity of the crystalline structure and morphology. The starting materials used in the mechanochemical method are mainly anhydrous ZnCl₂ and Na₂CO₃. NaCl is added to the system; this serves as a reaction medium and separates the nanoparticles. The zinc oxide precursor formed, ZnCO₃, is calcined at a temperature of 400–800 °C. The process as a whole involves the following reactions (1) and (2):



The mechanochemical method was proposed by Ao *et al.* they synthesized ZnO with an average crystallite size of 21 nm. The milling process was carried out for 6 h, producing ZnCO₃ as the zinc oxide precursor. Calcination of the precursor at 600 °C produced ZnO with a hexagonal structure. Tests showed that the size of the ZnO crystallites depends on the milling time and calcination temperature. Increasing the milling time (2–6 h) led to a reduction in the crystallite sizes (21.5–25 nm), which may indicate the existence of a “critical moment”. Meanwhile an increase in the calcination temperature from 400 to 800 °C caused an increase in crystallite size (18–35 nm).

The same system of reagents was used by Tsuzuki and McCormick. They found that a milling time of 4 h was enough for a reaction to take place between the substrates, producing the precursor ZnCO₃, which when calcined at 400 °C produced nanocrystallites of ZnO with an average size of 26 nm. Tsuzuki *et al.* showed that milling of the substrates without a thinner leads to the formation of aggregates measuring 100–1000 nm. This confirmed the important role played by sodium chloride in preventing agglomeration of the nanoparticles.

A milling process of ZnCl₂ and Na₂CO₃ was also carried out by Moballegh *et al.* and by Aghababazadeh *et al.* Moballegh *et al.*, investigated the effect of calcination temperature on particle size. An increase in the temperature of the process (300–450 °C) caused an increase in the size of the ZnO particles (27–56 nm). Aghababazadeh *et al.* obtained ZnO with an average particle size of approximately 51 nm and a surface area of 23 m²/g, carrying out the process at a temperature of 400 °C.

Stanković *et al.* extended their previous study to investigate mechanical-thermal synthesis (MTS)—mechanical activation followed by thermal activation of ZnO from ZnCl₂ and oxalic acid (C₂H₂O₄·2H₂O) as reactants with the intention of obtaining pure ZnO nanopowder. The study also aimed to examine the effects of oxalic acid as an organic PCA, and different milling times, on the crystal structure, average particle size and morphology of ZnO nanopowders. The mixture of initial reactants was milled from 30 min up to 4 h, and subsequently annealed at 450

°C for 1 h. Qualitative analysis of the prepared powders was performed using X-ray diffraction (XRD) and Raman spectroscopy. The XRD analysis showed perfect long-range order and the pure wurtzite structure of the synthesized ZnO powders, irrespective of the milling duration. By contrast, Raman spectroscopy indicates a different middle-range order of ZnO powders. From the SEM images, it is observed that the morphology of the particles strongly depends on the milling time of the reactant mixture, regardless of the further thermal treatment. A longer time of milling led to a smaller particle size. [6]

1.7.3 Chemical bath deposition

The chemical bath deposition technique mentioned above is simple, environmental friendly, and yields well-oriented ZnO nanorods at growth temperatures down to $\geq 90^\circ\text{C}$, at the same time it is suitable for large area growth. The growth procedures involve precoating the substrate with ZnO nanoparticles followed by a postgrowth 250°C annealing step. The coating layer acts as a preferential growth site during the growth process and also improves the *c*-axial orientation of the grown ZnO nanorods. The precoated substrate is then immersed in an aqueous solution coatings Zn precursor material and a pH adjusting chemical agent. In a few reports, the growth of ZnO NRAs was performed at a lower temperature down to 50°C , but either a high temperature treatment (300°C) for the precoating layer or the ZNRAs were grown as free-standing, that is, without a substrate. The growth of well-aligned ZNRAs at 50°C without any other heat treatment is of interest for the growth on flexible plastic substrates, for example, organic polymers on flexible plastic for hybrid white light emitting diodes (LEDs) applications. In addition, some other p-type substrates are of interest to be integrated with ZNRAs to form p-n heterojunctions. This is due to the lack of stable reproducible p-type doping for ZnO material. Examples of an interesting p-type substrate are copper oxides (CuO and Cu_2O) and organic semiconductors. Finally, metal layers are also of interest to be used as substrates for ZnO with the advantage of forming a contact at the bottom. Examples of interesting metals are silver (Ag) and copper (Cu). [3]

1.8 Crystal structure of ZnO

Crystalline ZnO has a wurtzite structure has a hexagonal unit cell with two lattice parameters, *a* and *c*, and belongs to the space group of C_{6v}^4 or $P6_3mc$. Figure 1 clearly shows that the structure is composed of two interpenetrating hexagonal closed packed (hcp) sublattices, in which each consist of one type of atom (Zn or O) displaced with respect to each other along the threefold *c*-

axis. Crystalline ZnO has a wurtzite (B4) crystal structure at ambient conditions. The ZnO can be simply explained schematically as a number of alternating planes stacked layer-by-layer along the c -axis direction and composed of tetrahedrally coordinated Zn^{2+} and O^{2-} . The tetrahedral coordination of ZnO gives rise to the noncentrosymmetric structure. In wurtzite hexagonal ZnO, each anion is surrounded by four cations at the corners of the tetrahedron, which shows the tetrahedral coordination and hence exhibits the sp^3 covalent-bonding.

Due to its vast areas of application, various synthetic methods have been employed to grow a variety of ZnO nanostructures, including nanoparticles, nanowires, nanorods, nanotubes, nanobelts, and other complex morphologies.

1.9 Nanoparticles of Zn

The tetrahedral coordination of Zn-O is shown. O atoms are shown as larger white spheres while the Zn atoms are smaller brown spheres.

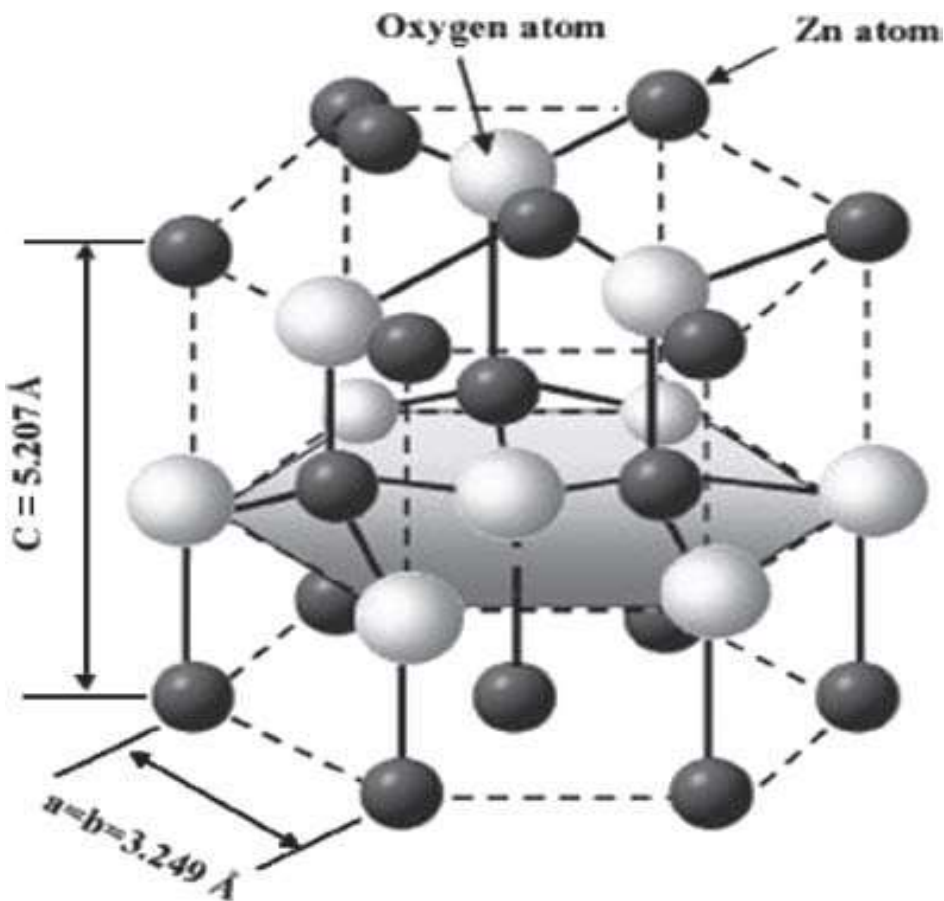


Figure 1.1 the hexagonal wurtzite structure model of ZnO.

1.10 Some factors affect on the morphology of ZnO nanoparticles

1-Reaction condition

2-Solvent.

3-A.cidic and basic solution rout.

4-Water addition.

5-Reactent concentration.

Synthesis of ZnO nanoparticles in the solution requires a well-defined shape and size of ZnO nanoparticles. In this regards, Monge et al reported room-temperature organometallic synthesis of ZnO nanoparticles of controlled shape and size in solution. The principle of this experiment was based on the decomposition of organometallic precursor to the oxidized material in air. It was reported that when a solution of dicyclohexylzinc(II) compound $[\text{Zn}(\text{c-C}_6\text{H}_{11})_2]$ in tetrahydrofuron (THF) was left standing at room temperature in open air, the solvent evaporated slowly and left a white luminescent residue, which was further characterized by X-ray diffraction (XRD) and transmission electron microscopy (TEM) and as agglomerated ZnO nanoparticles with a zincite structure having lack of defined shape and size.confirmed Monge et al. used a modified experimental condition using a ligand of long chain amine, i.e., hexadecylamine (HDA) under an argon atmosphere in addition to the above-mentioned solution, which resulted in well-defined ZnO nanoparticles. It was observed that shape, size, and homogeneity of the as-synthesized products depend upon various reactions conditions, i.e., the nature of the ligand, the relative concentration of reagents, the solvent, the overall concentration of reagents, the reaction time, the evaporation time, and the reaction/evaporation temperature. In addition, when a similar reaction .In addition, is carried out in dry air, it leads to agglomerated ZnO nanoparticles displaying no defined shape or size. In an elaborative manner, they analyzed that if the concentration of reagents in solution increases from 0.042 to 0.125 mol L⁻¹ nano-objects of higher aspect ratio will be formed. Exchanging THF for toluene or heptane produces nanoparticles of isotropic morphology with mean diameters of 4.6 for toluene and 2.4 nm for heptane.

A slow oxidation/evaporation process in THF (2 weeks) produces only very homogenous nanodisks having size 4.1 nm (Fig. 2(b)). Reducing the reaction time under argon to 5 min prior to oxidation leads to shorter nanorods $\sim 5.8 \times 2.7$ nm in size. Increasing the reaction temperature

leads to isotropic disk-shaped nanoparticles. Exchanging HDA for dodecylamine (DDA) or octylamine (OA) also leads to disks with mean diameters of 3.0 for DDA and 4.0 nm for OA (Figs.1.2(c and d)). In addition, nuclear magnetic resonance (NMR) studies confirmed that throughout the oxidation process, the amine ligand remains coordinated to zinc and suggested that this coordination participates in controlling the growth of ZnO nanoparticles. Kahn et al. reported the detailed experimental procedure based on the same synthetic route with different experimental parameters, i.e., the effects of solvent, ligand, concentration, time, and temperature. They explained that the reaction of organometallic complexes with oxygen or moisture leads exothermally to a hydroxide material, but in this case they did not observe any traces of hydroxide

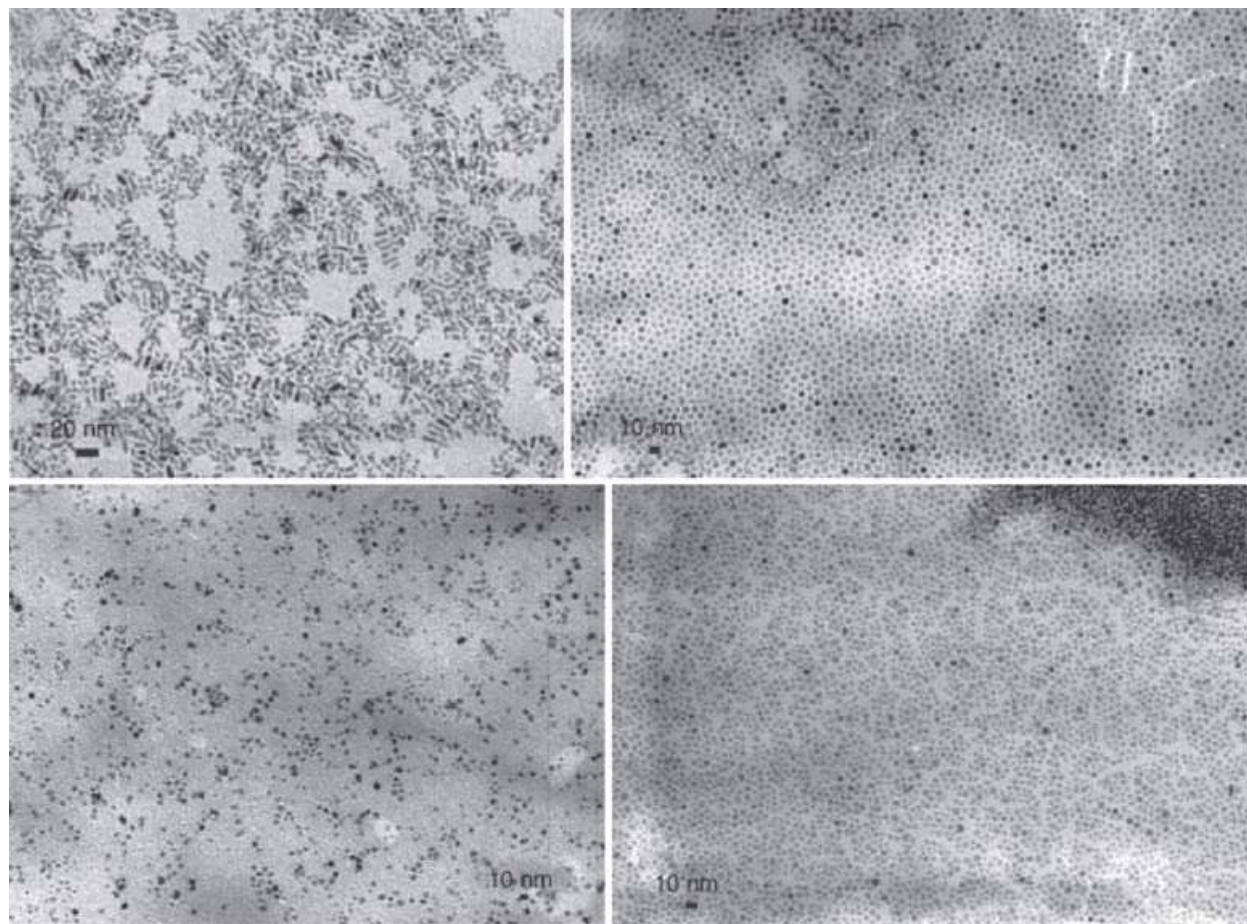


Figure 1.2. TEM micrographs of ZnO nanoparticles. (a) ZnO nanorods grown under standard conditions. (b) ZnO nanodisks following a slow oxidation/evaporation process in THF (2 weeks),

(c) ZnO nanodisks using DDA instead of HDA as the stabilizing ligand under standard conditions. (d) ZnO nanodisks using OA instead of HDA under standard conditions.

The solvent has an important effect on the morphology of ZnO nano-objec.

To show the effect of acidic and basic solution routes on the morphology of ZnO, Kawano et al. synthesized ZnO nanoparticles with various aspect ratios. In a typical synthetic process, ZnO grains and ZnO rods were obtained with various aspect ratios at 60°C with 2 h reaction in aqueous solution of ZnSO₄ *via* an acidic route (pH 5.6) with addition of NaOH and in a basic solution of NaOH *via* a basic route (pH 13.6) with addition of ZnSO₄, respectively. The observed aspect ratios were changed by this synthetic route, although the final pH of the solution was the same. The detailed morphological characterizations were performed by XRD, field emission scanning electron microscopy (FESEM), and field emission transmission electron microscopy (FETEM). XRD analysis confirmed the wurtzite ZnO type structures with peak broadening in the case of the acidic route compared to the basic route, which further confirmed the formation of smaller particles *via* the acidic route. FESEM images also confirmed the formation of ZnO particles and rods *via* acidic and basic routes, respectively. Further cumulative undersize distribution of precipitated ZnO particles confirmed that the particle shapes were spherical or ellipsoidal with diameters of 32 and 44 nm, respectively, *via* the acidic route at pH 12.8, which were consistent with the crystallite size calculated by Scherrer's formula using the (100) and (002) diffraction peaks observed in XRD spectra. Although the value of [OH⁻]/ [Zn²⁺] and the final pH were the same in the acidic and basic routes, the number of ZnO nuclei formed *via* the acidic route was deduced to be much higher than that obtained *via* the basic route because the degree of saturation at the initial stage of the acidic route was extremely high due to the low solubility of ZnO. Thus, most of the precursor species steeply precipitated as nanograins. On the other hand, ZnO nanorods formed in the basic route due to limitation of formed ZnO nuclei at the initial stage, and thus particle size increased *via* subsequent growth in the progressive stage.

To check the effect of water addition in the precursor-methanol solution for the morphological Evolution of ZnO particles, Wang et al. performed reactions based on hydrolysis of zinc acetate in methanol solvent at 60°C for 24 h and deposited over Al₂O₃ ceramic plate *via* the chemical deposition method. As the water/methanol volume ratio increased, the shape of the ZnO particles changed from irregular particles to plates and then from plates to regular cones, including the size change from nanoscale to micro-scale. In addition, if the volume of added water increased,

the height of the cones decreased. Addition of water controlled the hydrolysis of zinc acetate and affected the nucleation process of ZnO significantly. Moreover, addition of water can impede the [0001] growth and accelerate the [1100] growth if the volume ratio of added water/methanol is equal to or greater than 2:15. In this way, the shape and size of ZnO can be tailored by adjusting the volume ratio.

During the synthesis of ZnO nanoparticles, **the influences of the reactant concentration** were reported by Hu et al. In a typical process, ZnO nanoparticles were synthesized by using zinc acetate and NaOH in 2-propanol solution. As the nucleation and growth were fast in this synthetic process, at longer times the particle size was controlled by coarsening. In addition, coarsening kinetics were independent of the zinc acetate concentration from 0.5–1.25 mM at a fixed [zinc acetate: NaOH] ratio of 0.625. The width of the size distribution increased slightly with aging time. Moreover, if the zinc acetate concentration was fixed at 1 mM, the kinetics were independent of variation in the [zinc acetate: NaOH] ratio from 0.476–0.625. The presence of water in the reaction mixture was checked, and it was found that at low water concentration, the nucleation and growth of ZnO were very slow, which only slightly affected the coarsening kinetics for water content above ~20 mM. Thus, by this synthesis method, it is confirmed that ZnO nanoparticles are insensitive to the reactant concentration and presence of water.^[7]

The control of the shape and the orientation of nano-/ microcrystallites as well as the ability to order them into large three-dimensional arrays onto various types of substrates represent essential tasks to fulfill in order to create a future generation of smart and functional materials. Hitherto, the competence to generate aligned and ordered crystallites onto substrates was essentially based on template/membrane synthesis, patterning techniques, or epitaxial electrodeposition

Our strategy to control the shape and orientation of crystallites consists of growing thin-film materials directly onto substrates, from the molecular scale to the nano-/mesoscale, from aqueous precursors in solution by monitoring the thermodynamics and kinetics of nucleation and growth of the materials by controlling experimentally its interfacial tension. This approach led to the development of a novel general concept, namely, purpose built materials which is dedicated to the design of novel metal oxide materials with the appropriate morphology, texture, and orientation in order to probe, tune, and optimize their physical properties.

In most cases, homogeneous nucleation of solid phases (metal oxides in particular) requires a higher activation energy barrier, and therefore, heteronucleation will be promoted and will be energetically more favorable (e.g., influence of seeding on crystal growth). Indeed, the interfacial energy between crystals and substrates is usually smaller than the interfacial energy between crystals and solutions. Consequently, (hetero) nucleation takes place at a lower saturation ratio onto a substrate than in homogeneous solution. Epitaxial crystal growth occurs from substrate-generated nuclei along the easy direction of crystallization, and if the concentration of precursors is high, a condensed phase of single-crystalline rods perpendicular to the substrate is obtained. Recently, such approach has been successfully applied to the design of large arrays of three dimensional crystalline highly oriented hematite nanorod array, whose unique structural design led to a two-dimensional quantum confinement as well as an incident photon-to-electron conversion efficiency (IPCE) of 60% at 350nm. ^[8]

1.11 Characterization of zinc oxide nanoparticles

1.11.1 X-ray diffraction analysis

XRD diffraction pattern of ZnO nanoparticles was shown in **figure 1.3**. The peaks are indexed as 31.82° (100), 34.54° (002), 36.42° (101), 47.46° (102), 56.74° (110), 62.92° (103), 66.06° (200), 68.42° (112), 69.06° (201) and 78.82° (202) respectively. All diffraction peaks of sample correspond to the characteristic hexagonal wurtzite structure of zinc oxide nanoparticles ($a = 0.315$ nm and $c = 0.529$ nm). Similar, X-ray diffraction pattern were reported by C. Chen et. al. and Y. Pong et. al. Average particle size of ZnO nanoparticles is found to be 10.0 nm using Scherrer equation. Diffraction pattern corresponding to impurities are found to be absent. This proves that pure ZnO nanoparticles were as synthesized

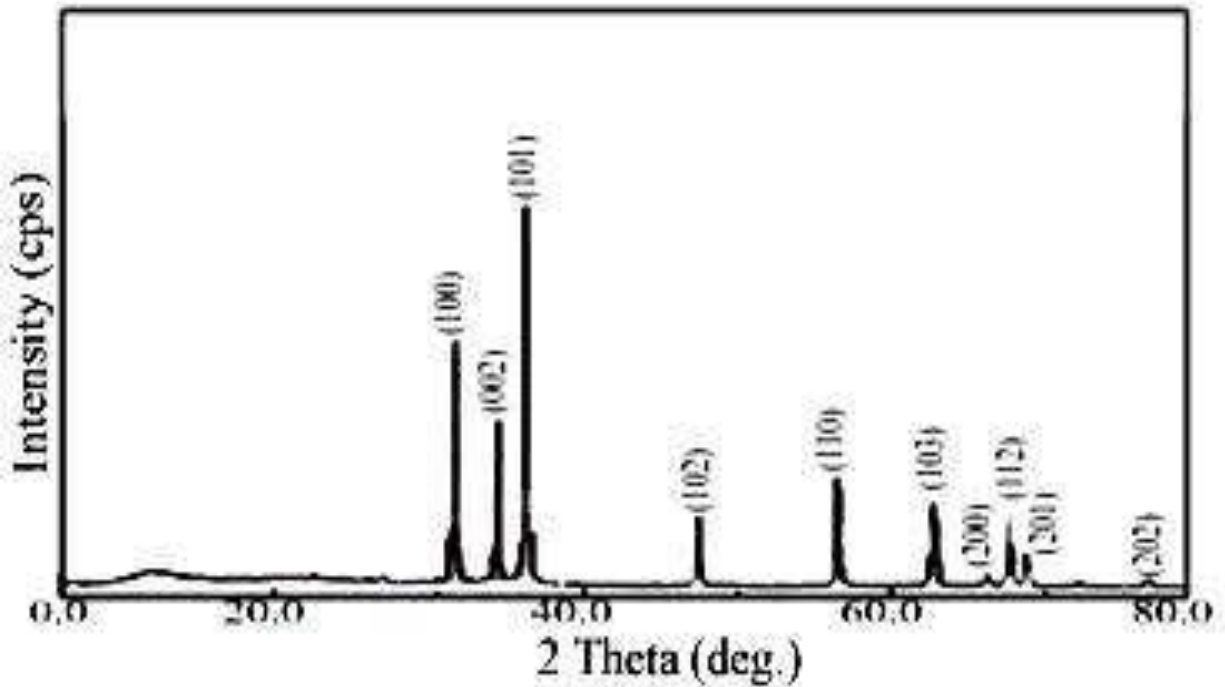


Figure 1.3. XRD patterns of ZnO nanoparticle

1.11.2 Transmission Electron Microscopy

TEM images of ZnO nanoparticles was shown in **figure 1.4**. Rod shape ZnO nanoparticles were observed in TEM images of average size in the range of 10.0-12.0 nm which is in the good agreement with the size calculated by XRD. Figure 2 (c) shows the selected area diffraction pattern (SAED) of ZnO nanoparticles. It shows that the particles are well crystallized. The diffraction rings on SAED image matches with the peaks in XRD pattern which also proves the hexagonal wurtzite structure of ZnO nanoparticles oparticles. Rod shape ZnO nanoparticles were observed in TEM images of average size in the range of 10.0-12.0 nm which is in the good agreement with the size calculated by XRD. **Figure 4** (c) shows the selected area diffraction pattern (SAED) of ZnO nanoparticles. It shows that the particles are well crystallized. The

diffraction rings on SAED image matches with the peaks in XRD pattern which also proves the hexagonal wurtzite structure

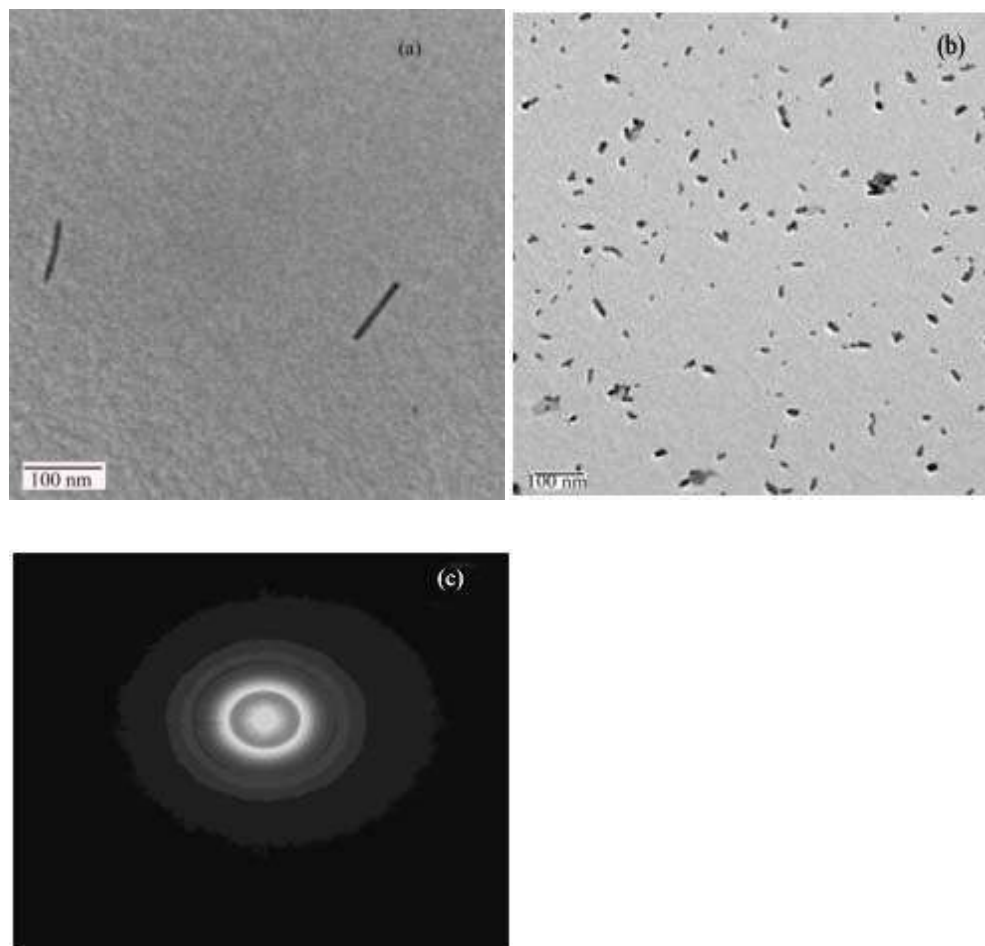


Figure 1.4. TEM images of ZnO nanoparticles (a, b) and its selected area electron diffraction image (c).

1.11.3 FTIR spectroscopy

FTIR spectra of ZnO nanoparticles was shown in **figure 1.5**. Infrared studies were carried out in order to ascertain the purity and nature of the metal nanoparticles. Metal oxides generally give absorption bands in fingerprint region i.e. below 1000 cm^{-1} arising from inter-atomic vibrations. The peak observed at 3452.30 and 1119.15 cm^{-1} are may be due to O-H stretching and deformation, respectively assigned to the water adsorption on the metal surface. The peaks at

1634.00, 620.93 cm^{-1} are correspond to Zn-O stretching and deformation vibration, respectively. The metal-oxygen frequencies observed for the respective metal oxides are in accordance with literature values V. Parthasarathi and G. Thilagavathi reported similar FTIR spectra observed of zinc oxide nanoparticles in their investigation.

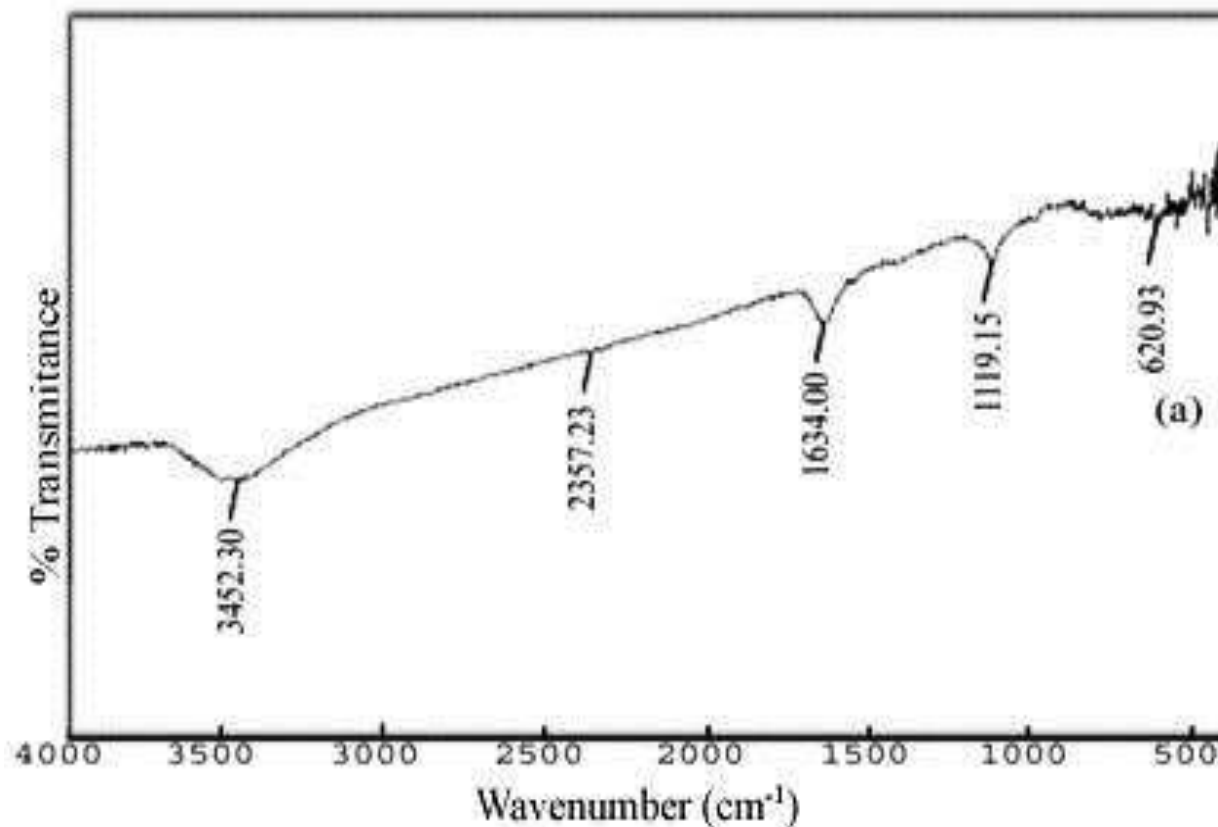


Figure1.5. FTIR spectra of ZnO nanoparticles

1.11.4 UV-Visible spectroscopy

The optical characterization of the sample was recorded on UV-Vis absorption spectrophotometer Figure 6 (a) shows the UV-Visible absorption spectra of ZnO nanoparticles as a function of wavelength. The UV-Visible absorption spectroscopy of ZnO nanoparticles in ethanol solvent shows an excitonic absorption peak at about 214 nm, which lies much below the band gap wavelength of 388 nm of bulk ZnO. The peak at ~214 nm is due to interband transition of copper electron from deep level of valence band. The blue shift in the peak centered at ~214

nm in absorption spectra (Figure 6 a) may be due to the transition of electrons from the more inner shell of copper to the uppermost shell as time passes. It is possible that, due to aggregation and agglomeration, particle size increases and material settled down on the bottom of container causing decrease in the absorbance. This behavior is typical for many semiconductors due to internal electric fields within the crystal and inelastic scattering of charge carriers by phonons. Absorption coefficient (α) associated with the strong absorption region of the sample was calculated from absorbent (A) and the sample thickness (t) was used the relation.

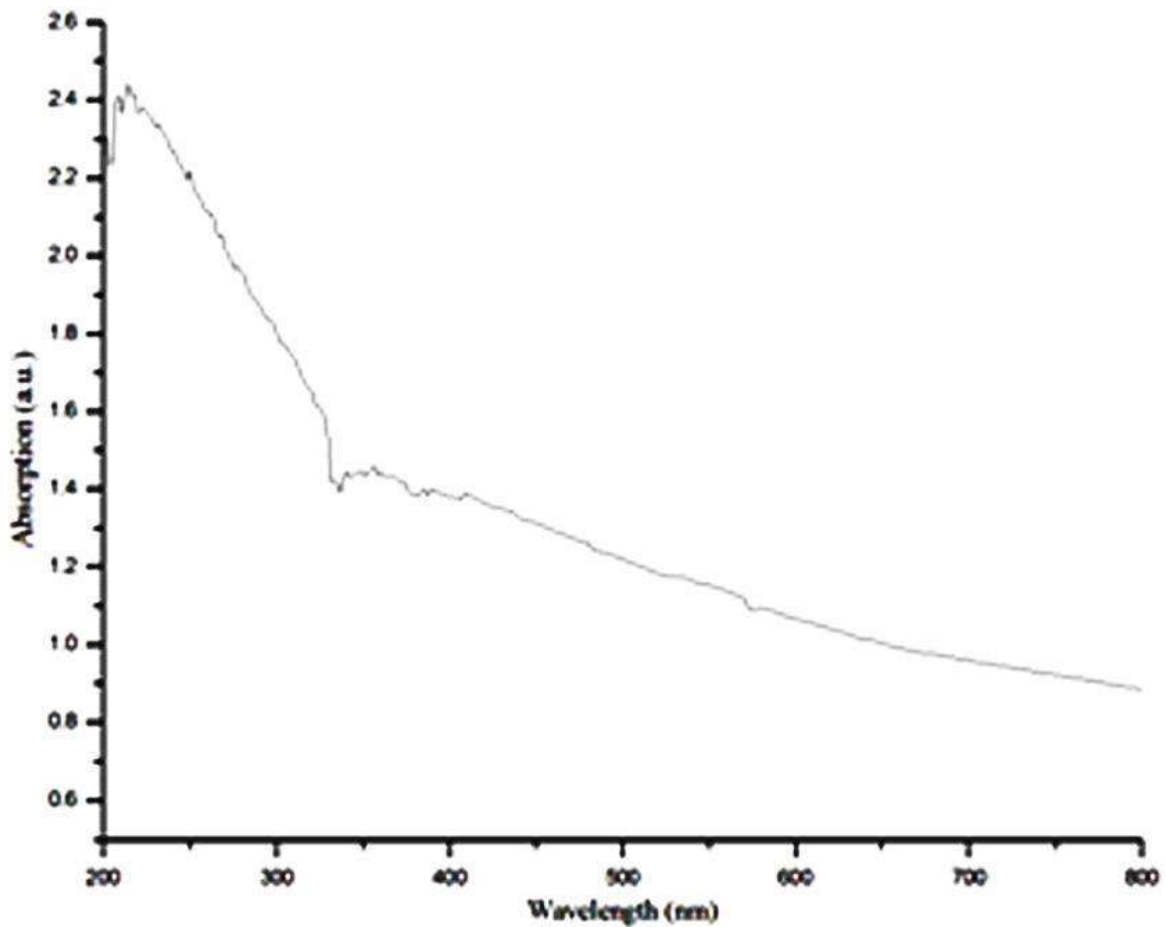


Figure1. 6. (a). Absorption of ZnO nanoparticles as a function of wavelength

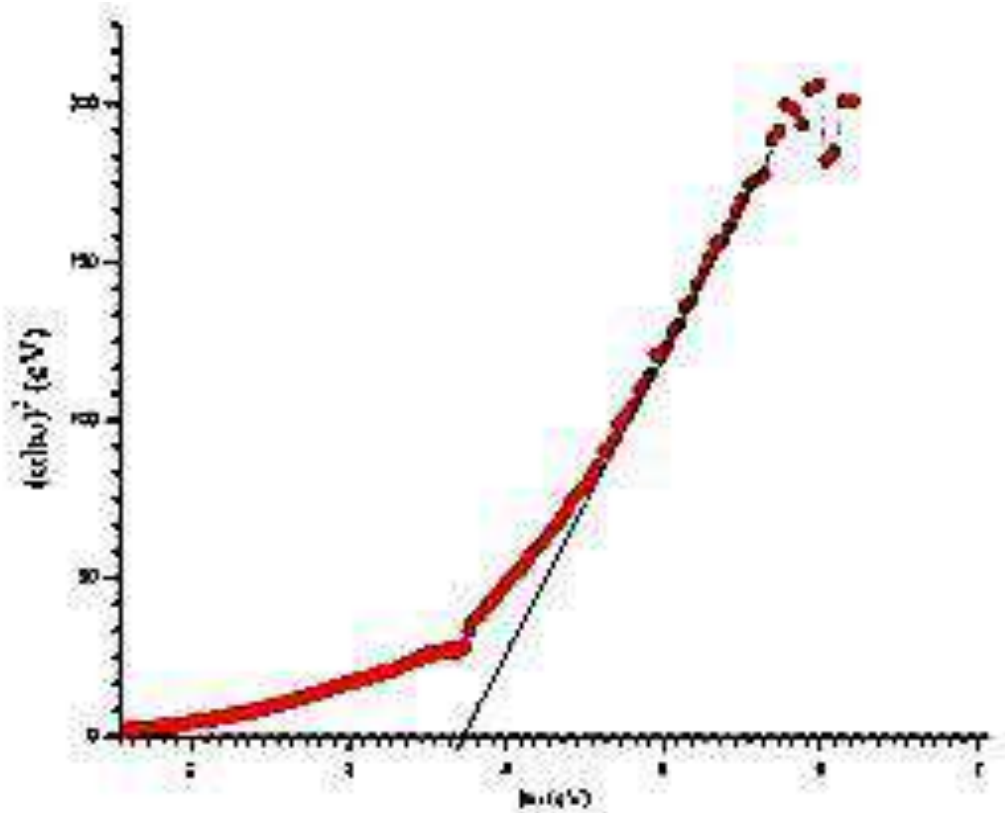


Figure 1. 6. (b). Variation of $(\alpha h\nu)^2$ with $h\nu$ for ZnO nanoparticles as a function of wavelength at n value of $1/2$

$$\alpha = 2.303A/t \quad (3)$$

While the optical band gap of ZnO nanoparticles is calculated using the Tauc relation

$$\alpha = B (h\nu - E_g)^n / h\nu \quad (4)$$

Where, α is the absorption coefficient, B is a constant, $h\nu$ is the energy of incident photons and exponents n whose value depends upon the type the transition which may have values $1/2$, 2 , $3/2$ and 3 corresponding to the allowed direct, allowed indirect, forbidden direct and forbidden indirect transitions, respectively. Figure 6 (b) show the variation of $(\alpha h\nu)^{1/n}$ vs. photon energy, $h\nu$ for ZnO nanoparticles with n values of $1/2$. Allowed direct band gap of ZnO nanoparticles is calculated to be 3.7 eV, which is higher than reported value 3.5348 eV. The increase in the band gap of the ZnO nanoparticles with the decrease in particle size may be due to a quantum confinement effect.

1.11.5. DSC analysis

The isothermal oxidation behavior and the oxidized structure of ZnO nanoparticles have been investigated using DSC technique over a temperature range of 50-600 °C in ambient air. Figure 5 shows DSC curve of zinc oxide nanoparticles. A small low temperature endothermic peak at 138.81 °C is due to loss of volatile surfactant molecule adsorbed on the surface of zinc oxide nanoparticles during synthesis conditions. A large high temperature endothermic peak at 260.43 °C is assigned the conversion of zinc hydroxide to zinc oxide nanoparticles. A small high temperature endothermic peak at 382.77 °C attributed the conversion of zinc oxide into zinc nanoparticles ^[9]

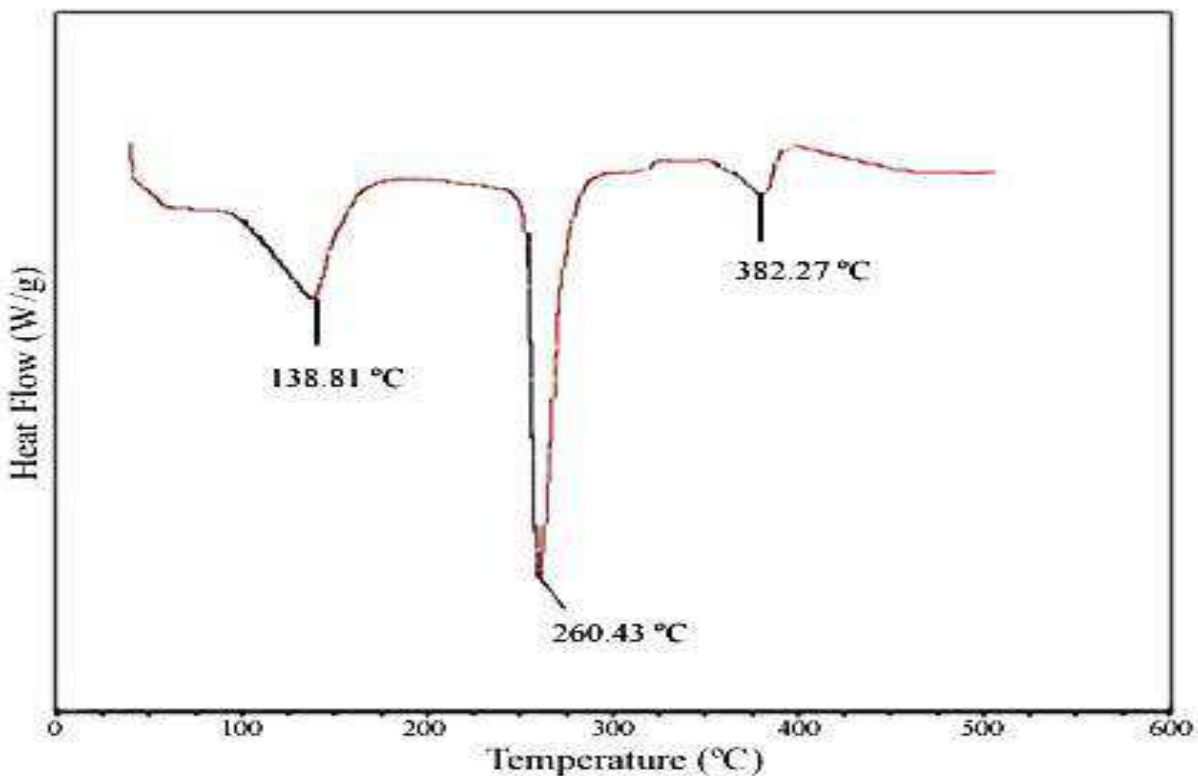


Figure1.7 DSC curve of ZnO nanoparticles.

1.12 Some applications of ZnO nanostructures

Because of its diverse properties, both chemical and physical, zinc oxide is widely used in many areas. It plays an important role in a very wide range of applications, ranging from tyres to ceramics, from pharmaceuticals to agriculture, and from paints to chemicals. **Figure1.9** summarized application paths of ZnO.

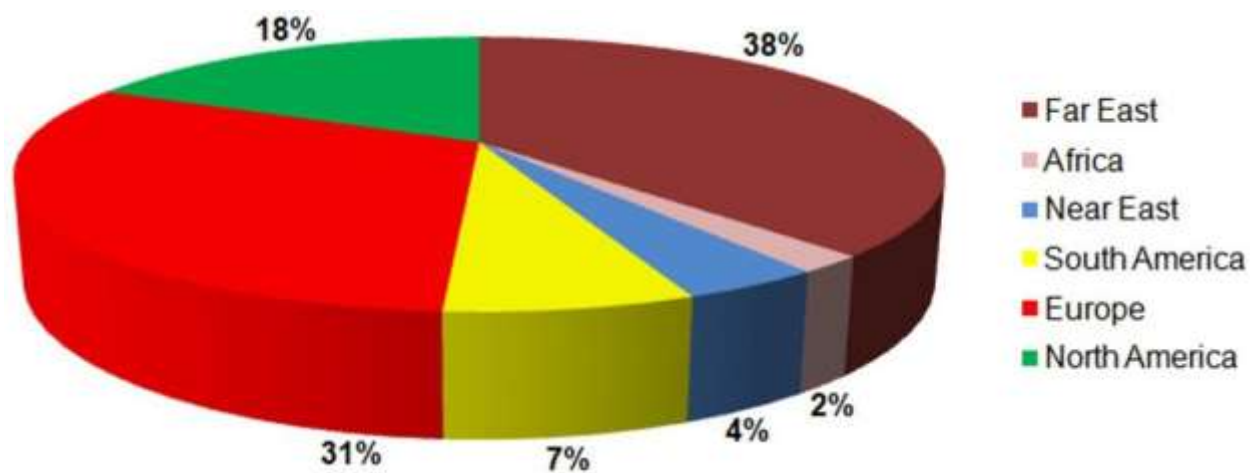


Figure1.8. Worldwide consumption of zinc oxide.

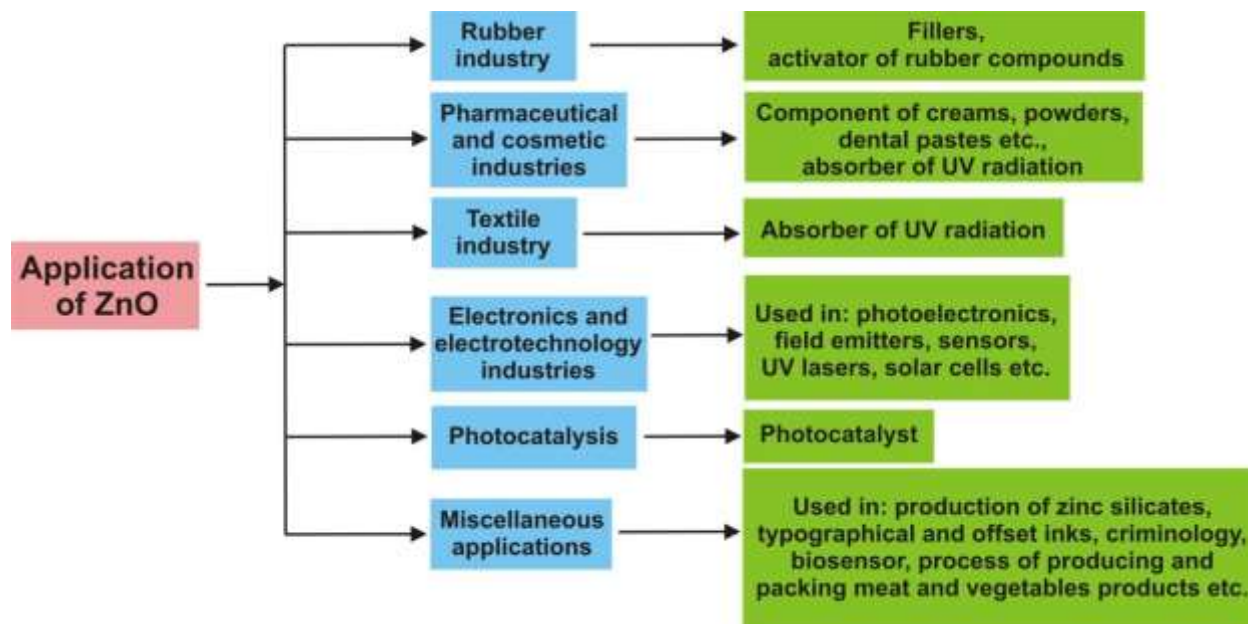


Figure 1.9. Schematic representation the application of ZnO. ^[6]

1.13 literature review

- A large fraction of the ZnO currently produced is used in the rubber and concrete industries. ZnO is an important additive to the rubber of car tyres. It has a positive influence on the vulcanisation process, and it considerably improves the heat conductivity, which is crucial to dissipate the heat produced by the deformation when the tyre rolls along the street. In concrete, an admixture of ZnO allows an increase in the processing time and improves the resistance of concrete against water. Other applications concern medicine or cosmetics. ZnO is used as an UV-blocker in suntan lotions or as an additive to human and Animals food. Furthermore, it is used as one component of mixed-oxide varistors, devices which allow voltage limiting.
- Due to its wide band gap, ZnO is transparent in the visible part of the electromagnetic spectrum. Highly n-doped ZnO: Al can therefore be used as a transparent conducting oxide (TCO). The constituents Zn and Al are much cheaper and less poisonous compared to the generally used indium tin oxide (ITO). One application which has begun to be commercially available is the use of ZnO as the front contact for solar cells, which avoids the shadow effect necessarily associated with metal-finger contacts. Other appearing applications use ZnO as the front contact of liquid crystal displays or ZnO: Al in the production of energy-saving or heat-protecting windows. A coating with TCO results in a

glass which lets the visible part of the spectrum in but either reflects the IR back into the room (energy saving) or does not let the IR radiation into the room (heat protection), depending on which side of the window has the TCO coating.^[10]

- .Using zinc oxide (ZnO) nanostructures, nanorods (NRs) and nanoparticles (NPs) grown on different substrates (submicrometer glass pipettes, thin silver wire and on plastic substrate) different bio-sensors were demonstrated. The demonstrated sensors are based on potentiometric approach and are sensitive to the ionic metals and biological analyte in question. For each case a selective membrane or enzyme was used. The measurements were performed for intracellular environment as well as in some cases (cholesterol and uric acid). The selectivity in each case is tuned according to the element to be sensed. Moreover we also developed photodynamic therapy approach based on the use of ZnO NRs and NPs. Necrosis/apoptosis was possible to achieve for different types of cancerous cell. The results indicate that the ZnO with its UV and white band emissions is beneficial to photodynamic therapy technology.
- ZnO possesses high Isoelectric Point (IEP) of 9.5 which makes it suitable for absorption of proteins with low IEPs where the protein immobilization is primarily driven by electrostatic interaction^[11]
- ZnO The fabrication and application of an intracellular K⁺ -selective microelectrode is demonstrated. ZnO nanowires with diameter of 100–180nm and a length of approximately 1.5µm are grown on a borosilicate glass microcapillary. The ZnO nanowires were coated by a K⁺ -ionophore-containing membrane. The K⁺ selective microelectrode exhibited a K⁺ -dependent potentiometric response versus an Ag/AgCl reference microelectrode that was linear over a large concentration range (25 µM–125 mM) with a minimum detection limit of 1 µM. The measured K⁺ concentrations in human adipocytes and in frog oocytes were consistent with values of K⁺ concentrations reported in the literature. The sensor has several advantages including ease of fabrication, ease of insertion into the cells, low cost, and high selectivity features that make this type of sensor suitable to characterize physiologically relevant ions within single living cells.^[12]
- An electrochemical biosensor based on ZnO nanorods for potentiometric cholesterol determination is proposed. Hexagon-shaped ZnO nanorods were directly grown on a silver wire having a diameter of 250 µm using low temperature aqueous chemical approach that

produced ZnO nanorods with a diameter of 125– 250 nm and a length of $\sim 1 \mu\text{m}$. Cholesterol oxidase (ChOx) was immobilized by a physical adsorption method onto ZnO nanorods. The electrochemical response of the ChOx/ZnO/Ag biosensor against a standard reference electrode (Ag/AgCl) was investigated as a logarithmic function of the cholesterol concentration ($1 \times 10^{-6} \text{ M}$ to $1 \times 10^{-2} \text{ M}$) showing good linearity with a sensitivity of 35.2 mV per decade and the stable output signal was attained at around 10 s .^[13]

- ZnO nanorods (NRs) with high surface area to volume ratio and biocompatibility is used as an efficient photosensitizer carrier system and at the same time providing intrinsic white light needed to achieve cancer cell necrosis. In this letter, ZnO nanorods used for the treatment of breast cancer cell (T47D) are presented. To adjust the sample for intracellular experiments, we have grown the ZnO nanorods on the tip of borosilicate glass capillaries (0.5 mm diameter) by aqueous chemical growth technique. The grown ZnO nanorods were conjugated using protoporphyrin dimethyl ester (PPDME), which absorbs the light emitted by the ZnO nanorods. Mechanism of cytotoxicity appears to involve the generation of singlet oxygen inside the cell. The novel findings of cell-localized toxicity indicate a potential application of PPDME-conjugated ZnO NRs in the necrosis of breast cancer cell within few minutes.^[14]
- ZnO nanorods were grown on a silver-coated tip of a borosilicate glass capillary (0.7 mm tip diameter) and used as selective potentiometric sensor of intracellular free Mg^{2+} . To functionalize the ZnO nanorods for selectivity of Mg^{2+} , a polymeric membrane with Mg^{2+} -selective ionophores were coated on the surface of the ZnO nanorods. These functionalized ZnO nanorods exhibited a Mg^{2+} -dependent electrochemical potential difference versus an Ag/AgCl reference microelectrode within the concentration range from 500 nM to 100 mM. Two types of cells, human adipocytes and frog oocytes, were used for the intracellular Mg^{2+} measurements. The intracellular concentration of free Mg^{2+} in human adipocytes and frog oocytes were 0.4–0.5 and 0.8–0.9 mM, respectively. Such type of nanoelectrode device paves the way to enable analytical measurements in single living cells and to sense other bio-chemical species at the intracellular level.^[15]
- We demonstrate hydrothermal synthesis of coral-like CuO nanostructures by selective growth on ZnO nanorods (NRs) at low temperatures. During the hydrothermal processing the resulting hydroxylated and eroded surface of ZnO NRs becomes favorable for the CuO

nanostructures growth via oriented attachments. Heterojunction p–n diodes fabricated from the CuO/ZnO nanocorals (NCs) reveal stable and high rectification diode properties with a turn-on voltage of ~ 1.52 V and a negligible reverse current. The humidity sensing characteristics of the CuO/ZnO NC diodes exhibit a remarkable linear (in a semilogarithmic scale) decrease in the DC resistance by more than three orders when the relative humidity is changed from 30–90%. The NC humidity sensor is also found to reveal the highest sensitivity factor of ~ 6045 among available data for the constituent materials and a response and recovery time of 6 s and 7 s, respectively.^[16]

- The inactivation of model microbes in aqueous matrix by visible light photocatalysis as mediated by ZnO nanorods was investigated. ZnO nanorods were grown on glass substrate following a hydrothermal route and employed in the inactivation of gram-negative *Escherichia coli* and gram-positive *Bacillus subtilis* in MilliQ water. The concentration of Zn^{2+} ions in the aqueous matrix, bacterial cell membrane damage, and DNA degradation at post-exposure were also studied. The inactivation efficiencies for both organisms under light conditions were about two times higher than under dark conditions across the cell concentrations assayed. Anomalies in supernatant Zn^{2+} concentration were observed under both conditions as compared to control treatments, while cell membrane damage and DNA degradation were observed only under light conditions. Inactivation under dark conditions was hence attributed to the bactericidal effect of Zn^{2+} ions, while inactivation under light conditions was due to the combined effects of Zn^{2+} ions and photocatalytically mediated electron injection. The reduction of pathogenic bacterial densities by the photocatalytically active ZnO nanorods in the presence of visible light implies potential ex situ application in water decontamination at ambient conditions under sunlight.^[17]
- We demonstrate intrinsic white light emission from hybrid light emitting diodes fabricated using an inorganic–organic hybrid junction grown at 50 °C on a paper substrate. Cyclotene was first spin coated on the entire substrate to act as a surface barrier layer for water and other nutrient solutions. The active area of the fabricated light emitting diode (LED) consists of zinc oxide nanorods (ZnO NRs) and a poly (9, 9-dioctylfluorene) (PFO) conducting polymer layer. The fabricated LED shows clear rectifying behavior and a broad band electroluminescence (EL) peak covering the whole visible spectrum range from 420 nm to 780 nm. The color rendering index (CRI) was calculated to be 94 and the correlated

color temperature (CCT) of the LED was 3660 K. The low process temperature and procedure in this work enables the use of paper substrate for the fabrication of low cost ZnO-polymer white LEDs for applications requiring flexible/disposable electronic devices.^[18]

1.14 Objectives of the study

1-preparation ZnO nanoparticles at low temperature.

2-To grow ZnO nanoparticles on glass substrate as a thin film.

3-To coat a thin film of ZnO nanoparticles which were grown on glass substrate by another layer of CuO nanoparticles.

4-To characterize of ZnO nanoparticles as a thin film on glass substrate.

5-To characterize of ZnO nanoparticles as a thin film on glass substrate coated by another layer of CuO nanoparticles.

Chapter two

Experimental

Chapter Two

Materials and Methods

2.1 Materials

2.1.1 Chemicals

- Zinc acetate dehydrate ($\text{Zn}(\text{CH}_3\text{COO})_2$) (assay 99.99%), density 1.84g/ml at 25°C (lit). impurities < 0.2% water. sigma Aldrich)
- Potassium hydroxide (KOH) (semiconductor grade, assay 99.99% basis trace metals basis, impurities 15% water, sigma Aldrich)
- Absolute methanol for (CH₃OH) (HPLC-PLUS -Gradient , assay 99.9%, CARLO ERBA)
- Zinc nitrate hexahydrate reagent grade ($\text{ZnNO}_3 \cdot 6\text{H}_2\text{O}$) (99.999% density 2.065g/ml at 25°C (lit), sigh)
- Hexamethylenetetramine ($\text{C}_6\text{H}_{12}\text{N}_4$) (assay $\geq 99.0\%$, grade ACS reagent, loss ≤ 2.0 loss on dry, sigma Aldrich)
- De ionized water

2.2 Instruments and equipments

2.2.1 Instruments

- Balance (BL3002, max=300g, d=0.01g).
- Hot plate stirrer (REMI 2MLH).
- Oven (super fit india)
- Scanning electron microscope .(JEOL, JSM-6380LA, resolution 3.0NM (30KV, WD8mm. SEI) (JEOL: japan electron optics laboratory)
- Uv –vis absorption spectrophotometer (JENWAY, model 6505 uv/vis spectrophotometer)

2.2.2 Equipments

Glass Beakers (250ml, 500ml) grade one, glass rode, stop watch, thermometer.

2.3 Preparation procedure

2.3.1 Seed solution for ZnO nanostructure growth

Zinc acetate dehydrate was mixed in absolute methanol (99%). then 0.01M concentration of zinc acetate dehydrate (274mg) was used in 125ml of methanol under stirring (the solution was transparent), it was heated to 60°C under continuous stirring. 109 mg of potassium hydroxide was dissolved in 65ml methanol (0.03M concentration), this solution was shaken well until it became transparent and added drop-wise to the heated solution of zinc acetate dehydrate under continuous stirring. the resulting solution was kept under stirring and heating (60°C) for 2 hours before it was become ready for use. some drops of the solution were put on the substrate and coat follow by spinning. Finally, the substrates (normal glass) were left to dry then cleaned with methanol.

2.3.2 The aqueous chemical growth solution for the ZnO

Zinc nitrate (zinc source salt) was added in 100 ml of deionized water (25 Mm). Hexamethylenetetramine (HMTA) in 100ml DI-water was added to solution one (the final ratio between the Zn concentration and HTMA was 1:1). The seeded substrates were loaded having its face down in the aqueous solution and then load the solution in side an oven heated at temperature 50-96°C for 4 hours. then the unloaded substrates (normal glass) were cleaned carefully in deionized water and dried them. Samples were become ready to characterization.

2.3.3 Standard cleaning procedure

Some acetone was pour on the substrates and shaken well for 1 minute, then was cleaned it with deionized water. The same steps was repeated using isopropanol. Finally the substrates was dried.

2.3.4 Coating ZnO with CuO

After the process of grown ZnO nanoparticles on glass substrates immediately were dip into equimolar solution of 0.025M copper nitrate pentahydrate and HMTA. After words the sample was kept into preheated oven at 80°C about 4 hours.

2.4 Characteraization methods

2.4.1Uv-vis absorption spectrophotometer test

Zinc oxide nanoparticles powder was dissolved in methanol, blank solution from methanol was used to calibrate the previous reading.

$$\alpha = 2.303A/t$$

While the optical band gap of ZnO nanoparticles is calculated using the Tauc relation

$$\alpha=B (hv -E_g)^n/hv$$

Where, α is the absorption coefficient, B is a constant, hv is the energy of incident photons and exponents n whose value depends upon the type the transition which may have values 1/2, 2, 3/2 and 3 corresponding to the allowed direct, allowed indirect, forbidden direct and forbidden indirect transitions, respectively.

Chapter three

Results and Discussion

Chapter Three

Results and discussion

ZnO nanoparticles which were prepared by hydrothermal method at low temperature (60 °C) were characterized by several techniques: UV-Vis absorption spectroscopy, scan electron microscope (SEM), energy dispersive X-ray spectroscopy (EDX)

3.1 UV –VIS absorption technique

3.1.1 The optical characterization of powder sample of ZnO recorded on Uv-Vis absorption spectrophotometer

ZnO in UV-Vis range of the electromagnetic spectra, is shown in **figure3.1** where a maxima is shown at 230nm. From the UV-Vis absorption data the band gap of ZnO was calculated using the relation

$$(\alpha h\nu)^2 = c (h\nu - E_g) \quad (1)$$

$$\alpha = B (h\nu - E_g)^{1/2}$$

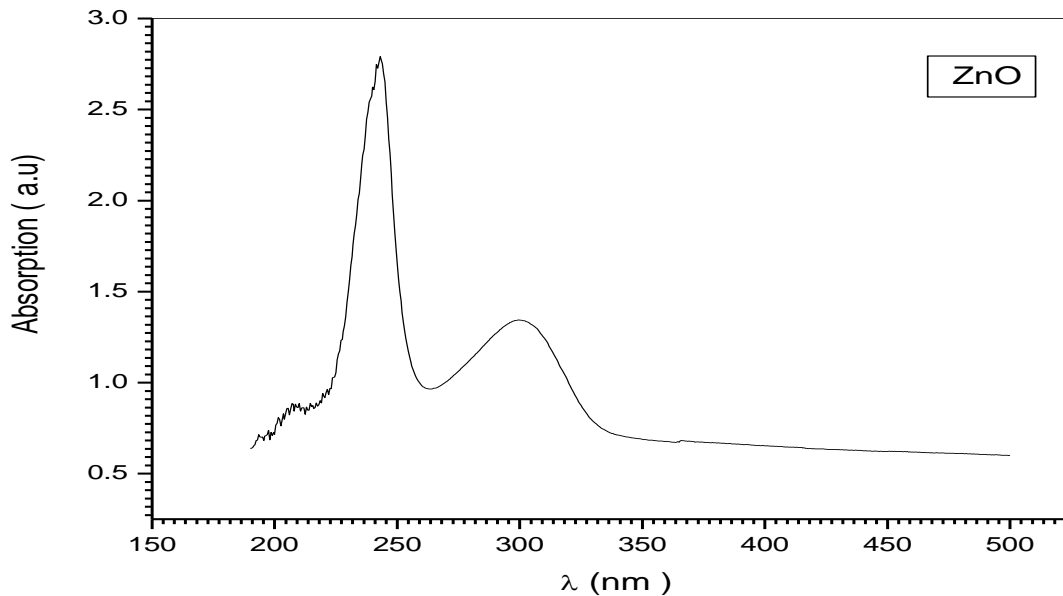


Figure.3.1. Absorption of ZnO nanoparticles as a function of wavelength

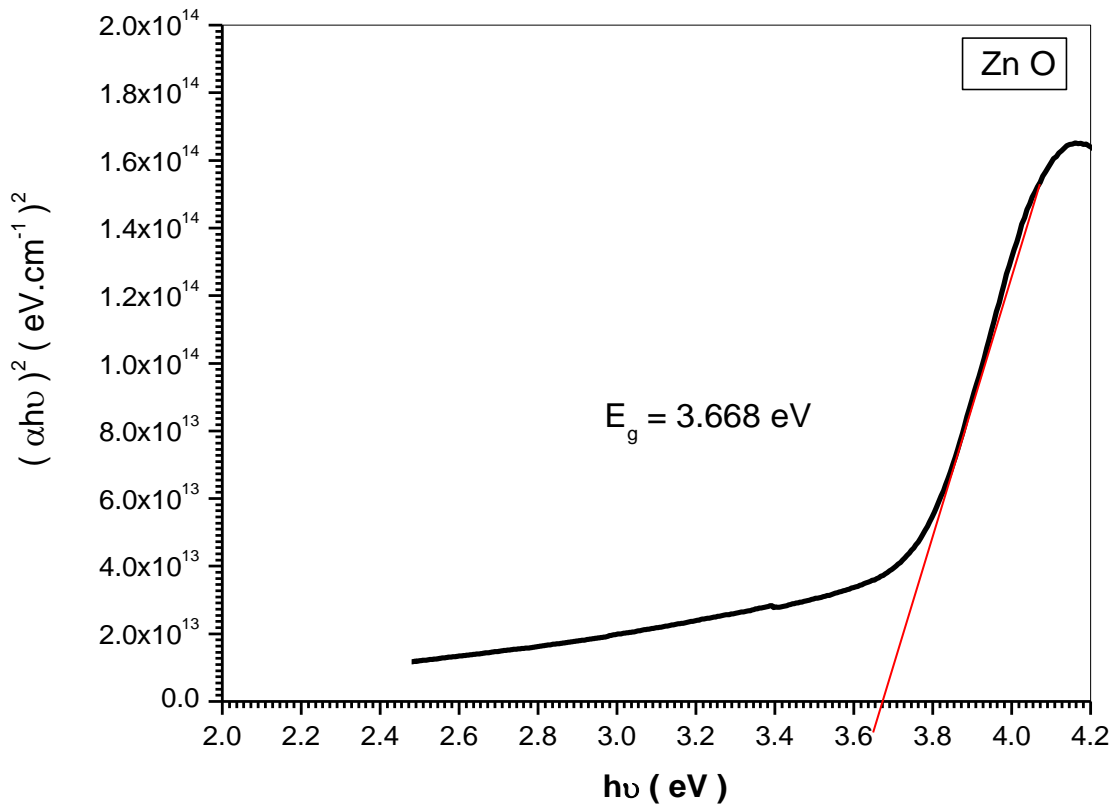


Figure 3.2 Variation of $(\alpha h\nu)^2$ with $h\nu$ for ZnO nanoparticles as a function of wavelength at n Value of 1/2.

$$(\alpha h\nu)^2 = c (h\nu - E_g)$$

Where c is constant. By plotting $(\alpha h\nu)^2$ vs photon energy ($h\nu$) and by extrapolating the straight line portion of curve to interpret the abscissa, the value of the energy band gap has been calculated and found to be $(E_g) = 3.668 \text{ eV}$

The increase of the band gap may be due to presence of impurities in the sample or elements which release electron

3.2 SEM technique

This test give information about sample's surface topology as shown in **figure 3.3**

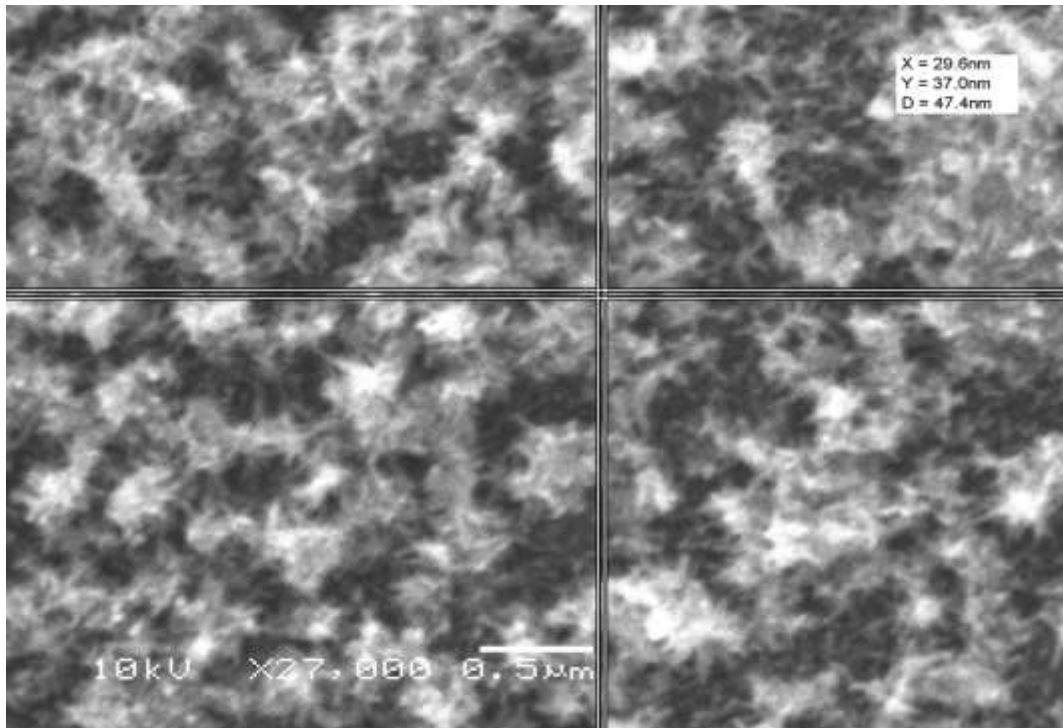


Figure3.3.SEM image of ZnO on normal glass

Figure3.3 shows SEM image that map the surface topology and shape of the ZnO nanoparticles on the glass substrate. The nanoparticles dimension are X=29.6nm, Y=37.0nm, distance between crystals D=47.4nm. It is clear that the grown ZnO particle were in the nanosized range in two dimension.

3.3 EDX technique

The number and energy of the x-ray emitted from a specimen can be measured by an energy – dispersive spectrometer

3.3.1 SEM plus EDX for ZnO on glass

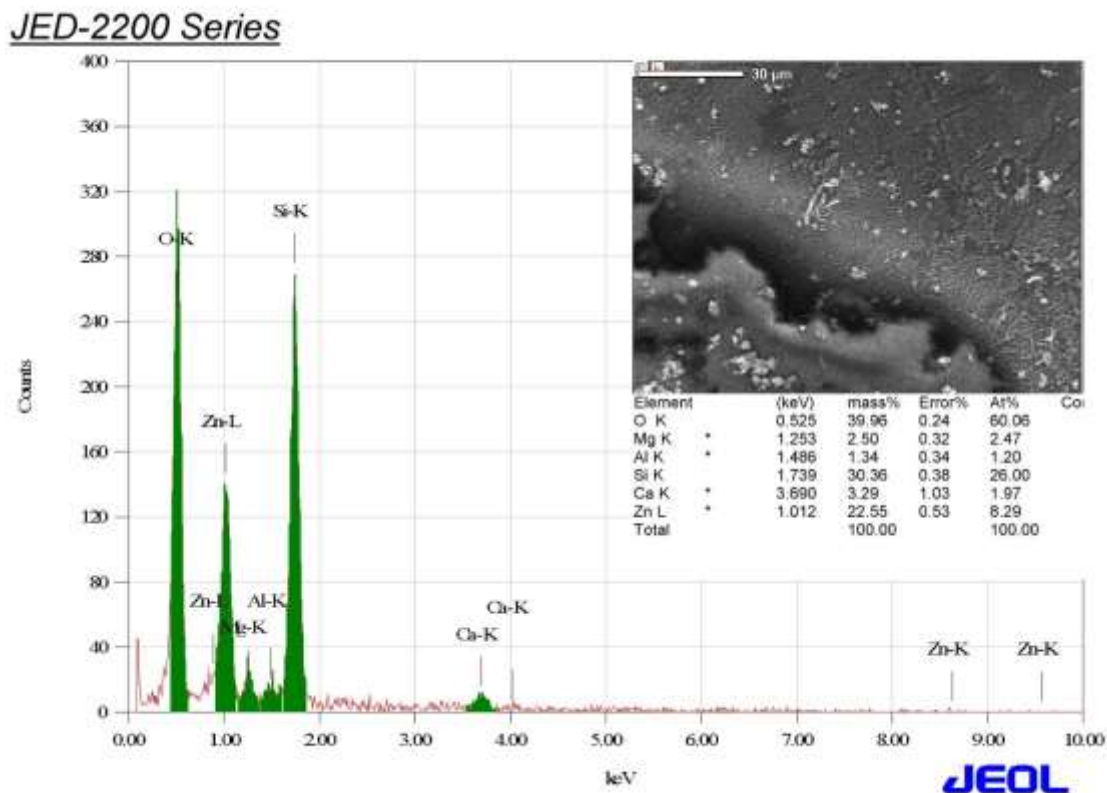


Figure3.4. SEM and EDX of ZnO on glass

Figure 3.4 shows that EDX profile of grown ZnO nanoparticles on the glass substrate .from the figure it clear that Zn and O were well presented .However, some other elements were also detected, namely Mg, Al, Si and Ca. These elements might be the impurities impeded in the glass substrate especially where there concentration is considered (Mg%=2.50%, Al%=1.34%, Si=30.36 %and Ca =3.29%). High percentage of Si indicate composition of substrate which

was made from glass. The presence of these elements as impurities may be the cause of the observed increase of the value of the band gap. The large width of the beaks in EDX profile shown in the figure indicate to nanosize of ZnO particles formation

3.2 SEM plus EDX result for ZnO coating by CuO

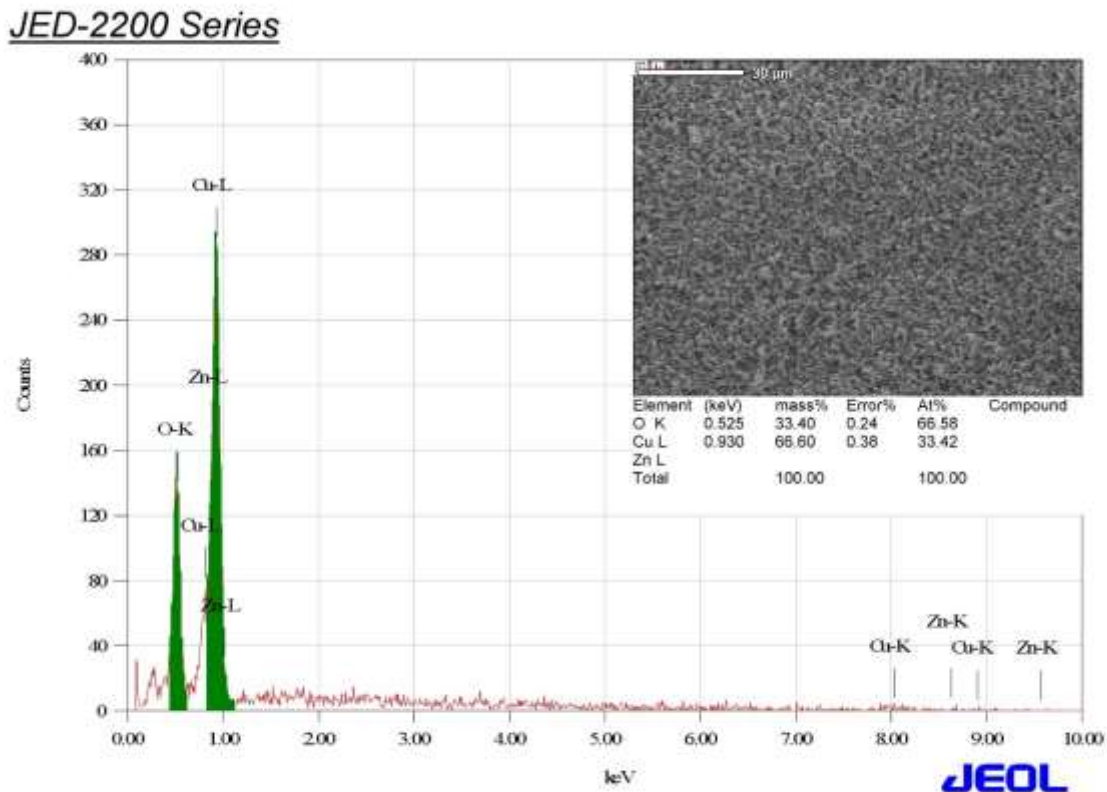


Figure3.5 SEM plus EDX of ZnO coating by CuO

Figure 3.5 shows the EDX profile of the CuO nanoparticles grown on ZnO nanoparticles on glass substrate. From the figure it is clear that Cu and O well present, however the layer of ZnO nanoparticles were also detected. Figure shows abroad and strong peak at 1.00KeV for Cu-L and Zn-L that means that ZnO nanoparticles were coated by CuO nanoparticles. Another sharp peaks at 8.00KeV, 8.80KeV, 9.00KeV, 9.60Kev indicate the presence of CuO and ZnO particles out of

nanosize range, as a result the sample contain two type of particles one of them on the range of nanosize and the other is out of range. The absence of Mg, Al, Ca and Si from EDX profile indicate that CuO and ZnO were grown on glass substrate as consecutive formed hence the radiation penetrates the CuO layer to ZnO layer without reach to the glass substrate

3.5 Effect of temperature on shape and size of ZnO nanoparticles

Temperature had direct effect on the particles size and shape. It lead to agglomeration of the particles as was shown on **figure3.6**

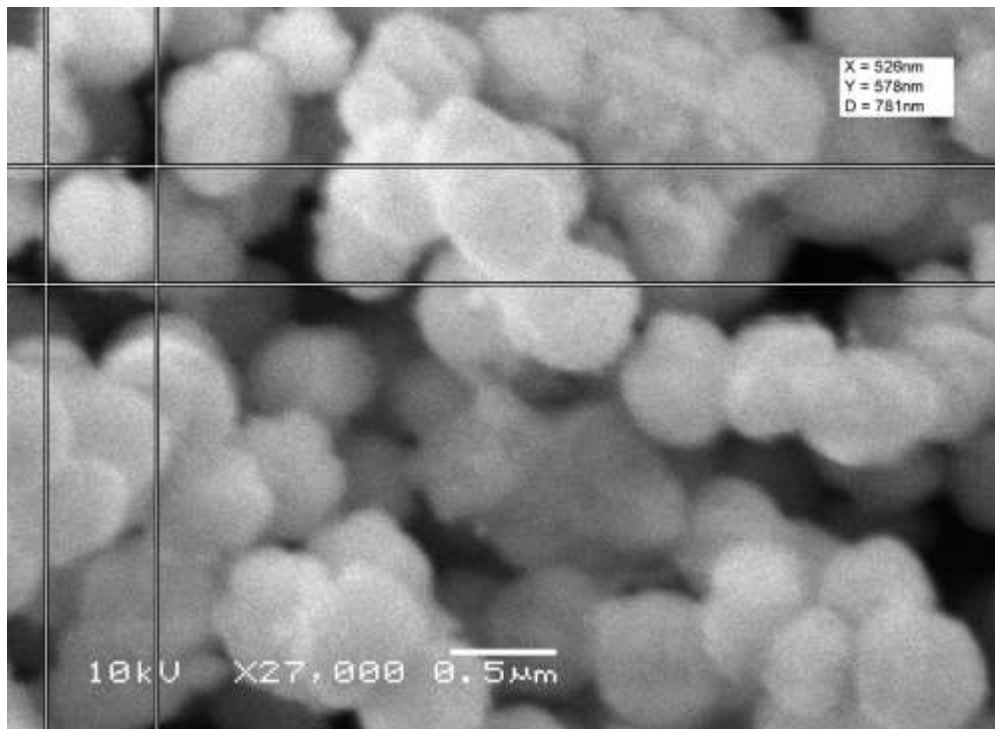


Figure3.6 SEM image for ZnO Coating by CuO on normal glass.

Figure 3.6 shows the SEM image that map surface topology and shape of CuO nanoparticles grown on ZnO nanoparticles on glass substrate. The nanoparticles dimensions are X=520nm, Y=575nm and the distance between crystals D=781nm. It is clear that the CuO particles grown

on ZnO particles were out of nanosize range .This may be due to arising temperature over (60°C) on the oven. .which results in particles agglomeration as shown in **figure 3.6**

.A lot of work has been done in the area of transition metal doping of ZnO single crystals and thin films. However, a few reports on the synthesis and characterization of ZnO nanostructures doped with different impurities like Al, Sn, Ga, In, Sb, Cu, etc. are available in the literature. Li *et al*] has synthesized ZnO nanorods doped with manganese (Mn), chromium (Cr) and cobalt (Co) in a hydrothermal synthesis using zinc nitrate, transition metal nitrate an hexamethylenetetramine. It was observed that the doping was good with Mn (8% doping from a 10% solution) and Co (17% doping from a 10% solution) dopants and poor with Cr (4% doping from a 10% solution). The morphology of the doped ZnO nanorods was different from that of the un doped nanorods ^[5]

3.6 conclusion

It was found that hydrothermal method at low temperature is effective method to synthesis ZnO nanoparticles and grown it on glass substrates and coated by another layer of nanoparticles. Creating particle by this size (nano) needed cautions like well controlling on temperature at (60° C). Rising temperature over (60°C) has direct affect on particles size and lead to agglomeration.

References

- [1] Pal S.I., Jan., Manna P.K., Mohanta G.P., Manavalan R., (2011),” An overview of preparation and characterization”, *Journal of Applied Pharmaceutical Science*, **1** (6): 228-234.
- [2] Willander M., Ul Hasan K., Nur O., Zainelabdin A., Zaman S. and Amin G., (2012) ,” Recent progress on growth and device development of ZnO and CuO nanostructures and graphene nanosheets”, *Journal of Materials Chemistry*, **22**: 2337–2350.
- [3] Zainelabdin A., Zaman S., Amin G., Nur O., and Willander M., (2010),” Deposition of Well-Aligned ZnO Nanorods at 50 °C on Metal, Semiconducting Polymer, and Copper Oxides Substrates and Their Structural and Optical Properties”, *Crystal Growth & Design*, **10**:3250 - 3256.
- [4] Dinh C.T., Nguyen T.D. Kleitz F., and Do T.O. (2012), “Shape-Controlled Synthesis of Metal Oxide Nanocrystals”, *Controlled Nanofabrication's: Advances and Applications*, 328-367.
- [5] Baruah S. and Dutta J., (2009), “Hydrothermal growth of ZnO Nanostructures”, *science and technology of advanced materials*, **10**:1 -18.
- [6] Kołodziejczak-Radzimska A. and Jesionowski T., (2014),” Zinc Oxide—From Synthesis to Application”, *materials*, **7**:2831-2881.
- [7] Umar A. and Hahn Y.-B., (2010), “Metal Oxide Nanostructures and Their Applications”, Vaseem M., Umar A. and Hahn Y.-B.,”ZnO Nanoparticles: Growth, Properties, and Applications” , *American Scientific Publishers*, **5**:1-36.
- [8] Vayssieres L., Keis K., Lindquist S.-E., and Hagfeldt A., (2001),”Purpose-Built Anisotropic Metal Oxide Material: 3D Highly Oriented Microrod Array of ZnO”, *J. Phys. Chem*, **105**:3350-3352.
- [9] Kumar H., Rani R., (2013),”Structural and Optical Characterization of ZnO Nanoparticles Synthesized by Microemulsions Route”, *International Letters of Chemistry, Physics and Astronomy*, **14**:26-36.
- [10] Prof. Dr. Klingshirn C., (2007),” ZnO: Material, Physics and Applications”, *ChemPhysChem*, **8**:782 – 803.
- [11] Willander M., Nur O., Fakhar-e-Alam M., Sadaf J.R, Israr M.Q, Sultana K., Ali S. M. U, Asif M.H, (2011),”Applications of Zinc Oxide Nanowires for Bio-photonics and Bio-electronic”, *Oxide-based Materials and Devices II*, **7940** :79400F1-13.

- [12] Ali S.M.U., Member S., *ieee*, Muhammad H. Asif, Fulati A., Nur O., Willander M., Brännmark C., Strömfors P., Ulrika H. Englund, Elinder, and Danielsson B.,(2011),”Intracellular K⁺ Determination With a Potentiometric Microelectrode Based on ZnO Nanowires”,*ieee transactions on nanotechnology*, **10** : 913-919.
- [13] IsrarM.Q., SadafJ.R., M.H. Asif., Nur O., Willander M, Danielsson B , (2010),”Potentiometric cholesterol biosensor based on ZnO nanorods chemically grown on Ag wire”,*Thin Solid Films*,**519**:1106-1109.
- [14] Kishwar S., Asif M.H., Nur O., Willander M., Larsson P-O., (2010),“Intracellular ZnO Nanorods Conjugated with Protoporphyrin for Local Mediated Photochemistry and Efficient Treatment of Single Cancer Cell”, *springer*, **5**:1669–1674.
- [15] Asif M.H., Ali S.M.U., Nur O., Willander M., Englund U.H., Elinder F., (2010), “Functionalized ZnO nanorod-based selective magnesium ion sensor for intracellular measurements”, *Biosensors and Bioelectronics*, **26**:1118-1123.
- [16] Zainelabdin A., Amin G., Zaman S, Nur O., Lu.J, Hultmanb L. and Willander M,(2012), “CuO/ZnONanocorals synthesis via hydrothermal technique: growth mechanism and their application as Humidity Sensor”, *Journal of Materials Chemistry*,**22**:11583–11590.
- [17] |Sapkota A., Anceno A.J, Baruah S, ShipinO.V and Dutta J., (2011), “Zinc oxide nanorod mediated visible light photoinactivation of model microbes in water”, *nanotechnology*, **22**:1-7.
- [18] Amin G., Zaman S., Zainelabdin A., Nur O., and Willander M., (2010), “ZnO nanorods–polymer hybrid white light emitting diode grown on a disposable paper substrate”, *phys. Status Solidi RRL* **5**, **2**:71-73.
- [19] AlJaumaili H.S. and Al rawi K., (2011),” effect of thermal annealing and laser radiation on the optical properties of AgAIS thin films”, *iraqi journal of physics*, **9**:79-83.